AN ODD ANALOG OF PLAMENEVSKAYA'S INVARIANT OF TRANSVERSE KNOTS

by

GABRIEL MONTES DE OCA

A DISSERTATION

Presented to the Department of Mathematics
and the Graduate School of the University of Oregon
in partial fulfillment of the requirements
for the degree of
Doctor of Philosophy

September 2020

DISSERTATION APPROVAL PAGE

Student: Gabriel Montes de Oca

Title: An Odd Analog of Plamenevskaya's Invariant of Transverse Knots

This dissertation has been accepted and approved in partial fulfillment of the requirements for the Doctor of Philosophy degree in the Department of Mathematics by:

Robert Lipshitz	Chair
Daniel Dugger	Core Member
Nicholas Proudfoot	Core Member
Micah Warren	Core Member
James Brau	Institutional Representative

and

Kate Mondloch	Interim Vice Provost and Dean of the Graduate School

Original approval signatures are on file with the University of Oregon Graduate School.

Degree awarded September 2020

DISSERTATION ABSTRACT

Gabriel Montes de Oca

Doctor of Philosophy

Department of Mathematics

September 2020

Title: An Odd Analog of Plamenevskaya's Invariant of Transverse Knots

Plamenevskaya defined an invariant of transverse links as a distinguished class in the even Khovanov homology of a link. We define an analog of Plamenevskaya's invariant in the odd Khovanov homology of Ozsváth, Rasmussen, and Szabó. We show that the analog is also an invariant of transverse links and has similar properties to Plamenevskaya's invariant. We also show that the analog invariant can be identified with an equivalent invariant in the reduced odd Khovanov homology. We demonstrate computations of the invariant on various transverse knot pairs with the same topological knot type and self-linking number.

CURRICULUM VITAE

NAME OF AUTHOR: Gabriel Montes de Oca

GRADUATE AND UNDERGRADUATE SCHOOLS ATTENDED:

University of Oregon, Eugene, OR
Lewis & Clark College, Portland, OR

DEGREES AWARDED:

Doctor of Philosophy, Mathematics, 2020, University of Oregon
Bachelor of Arts, Mathematics, 2011, Lewis & Clark College

AREAS OF SPECIAL INTEREST:

Low Dimensional Topology, Mathematical Relativity, Partial Differential Equations

PROFESSIONAL EXPERIENCE:

Graduate Employee, University of Oregon, 2012-2020

ACKNOWLEDGEMENTS

I would like to thank my advisor Robert Lipshitz, without whose support, feedback, encouragement, insight, and patience, this dissertation would not have been possible.

I also thank the Department of Mathematics, Robert Lipshitz, Daniel Dugger, and Nicholas Proudfood for their support through the myriad logistical and extraordinary obstacles faced in the course of my study.

I am forever grateful to my husband, Josh Francis, for his unerring support throughout this endeavor and beyond. To Preston Bentley, my family Carlos, Deborah and Alex, and my friends Jessica, Chris, Gavin, and Clover, I thank them for their support, encouragement and continued faith in me.

This research was supported in part by NSF grant DMS-1560783.

For Josh.

TABLE OF CONTENTS

Chapter Page

Chapter Page

LIST OF FIGURES

Figure Page

CHAPTER I

INTRODUCTION

1.1. Knots and Braids

A *knot* is a smooth embedding of a circle in $\mathbb{R}^3$ (or in S^3). Two knots K and K' are *isotopic* if there is a smooth one-parameter family of embeddings containing both. We consider knots up to isotopy. A *knot diagram* is a projection of a knot onto the plane that is an immersion arranged so that no more than two points of the knot are in the preimage of a point in the projection and at such double points (called *crossings*), the two segments in a neighborhood of that point intersect transversely. Relative to the projection, one segment of the knot crosses "over" the other at a crossing. In a knot diagram, this segment is drawn with a solid line crossing over a broken segment, which passes under. See Figure 1.

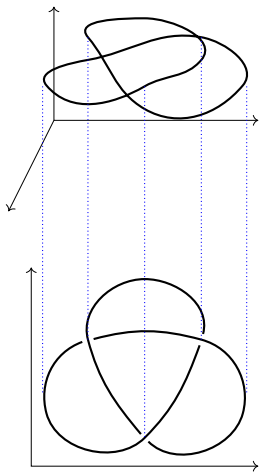

FIGURE 1. **A projection of a trefoil knot to a knot diagram.**

Theorem 1 (Alexander-Briggs [AB27], Reidemeister [Rei27])**.** *Two knot diagrams D and D' are diagrams of the same knot if they are related by isotopies of $\mathbb{R}^2$ and a finite sequence of the three Reidemeister Moves: RI, RII, and RIII. See Figure 2.*

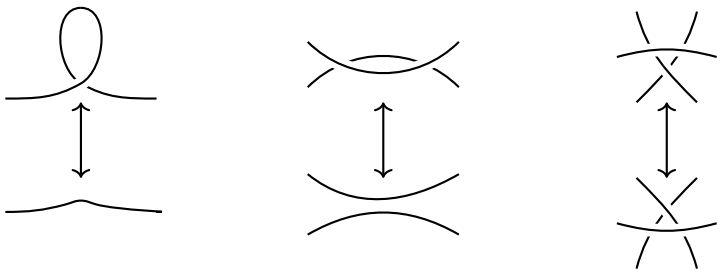

FIGURE 2. **The three Reidemeister moves.**

A multi-component knot is called a *link*. That is, a link is an embedding of a disjoint union of circles in $\mathbb{R}^3$ (or S^3). Link isotopy and link diagrams are defined similarly to knot isotopy and knot diagrams, and Theorem 1 holds for links as well.

An *oriented knot* is a knot that has been given an orientation. Equivalently, if we view a knot as a smooth closed path with nonvanishing derivative, an orientation on the knot comes from the direction of its derivative. In diagrams, we will denote the orientation of a knot with an arrow. An *oriented link* is a link whose components are oriented.

We can give signs to the crossing of an oriented link according to Figure 3. In a knot, the sign of a crossing is independent of the orientation since reversing the orientation of a knot reverses both of the arrows and thus produces a 180-degree rotation of the crossings in Figure 3. However, since crossings in a link diagram could have segments from two different components, if we change the orientation on only one of those components, we change the sign of the crossing. An *alternating*

knot is a knot that has a diagram such that along its path, the curve strictly alternates between passing over and under itself at each crossing.

FIGURE 3. **Crossing signs.**

The *inverse* of an oriented knot K, denoted $\overline{K}$ is the oriented knot with the same image but opposite orientation. A knot is called *reversible* if there is an isotopy from K to $\overline{K}$. Given a knot K, its *mirror* mK is a knot such that there is an orientation-reversing homeomorphism between $(\mathbb{R}^3, K)$ and $(\mathbb{R}^3, mK)$. In a diagram, the mirror of a knot arises from switching which segment goes over and which goes under at every crossing. To be clear, the inverse of the knot reverses the intrinsic one-dimensional orientation of the knot, while the mirror of the knot reverses the ambient three-dimensional orientation. A knot is called *amphichiral* if it is isotopic to its mirror, and *chiral* if it is not.

Given two oriented knots K_1 and K_2 we can produce a new oriented knot, their *connected sum* $K_1 \# K_2$, by removing a segment from each K_1 and K_2 and then gluing the ends together according to their orientations. See Figure 4. The connected sum of knots is both associative and commutative. Without specifying components, the connected sum of two links is not well defined. A knot K is *prime* if $K = K_1 \# K_2$ implies either K_1 or K_2 is the unknot.

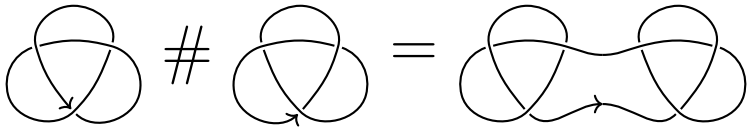

FIGURE 4. **The connected sum of the left and right trefoil knots.**

Given two knot diagrams, it is not necessarily obvious if they represent the same knot. To distinguish knots, a number of algebraic invariants have been defined. Some invariants are easy to define but not easy to compute. For example, the *crossing number* of a knot is the minimal number of crossings needed in a diagram representing that knot. However, given a diagram of a knot, it is not always clear if some sequences of Reidemeister moves will produce a diagram with fewer crossings. A knot invariant is called *effective* if there is a pair of knots that it distinguishes.

The Kaufmann bracket is an invariant of link diagrams, which assigns to each diagram a Laurent polynomial in q. The Kauffman bracket of the empty link is defined to be

$$\langle \emptyset \rangle = 1.$$

The Kaufmann bracket of the disjoint union of the trivial unknot diagram O and a diagram D is defined to be

$$\langle O \sqcup D \rangle = (q + q^{-1})\langle D \rangle.$$

Fixing a crossing in D, we can produce two related diagrams D_0 and D_1, where the fixed crossing in D is replaced by the smoothings as shown in Figure 5. We can then define the Kaufmann bracket on D recursively by the following skein relation,

$$\langle D \rangle = \langle D_0 \rangle - q\langle D_1 \rangle.$$

The Kauffman bracket fails to be a link invariant because it is not invariant under type I and II Reidemeister moves. The difference is a factor of a power of q and a

sign. However, the RI move also introduces either a positive or a negative crossing, and the RII move introduces both one positive and one negative crossing. The crossings are added in such a way that we can compensate for the differences these moves introduce.

Given a link L with diagram D that has n_+ positive crossings and n_- negative crossings, the (unreduced) Jones polynomial, defined as

$$\hat{J}(L) = (-1)^{n_-} q^{n_+ - 2n_-} \langle D \rangle,$$

is a link invariant. The Jones polynomial is useful because, in addition to being an effective link invariant, its value provides a necessary condition for a link to be chiral, and it puts a lower bound on a link's crossing number.

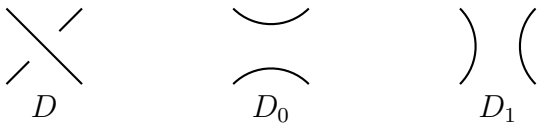

FIGURE 5. **The smoothings for defining the Kauffman bracket.**

A *braid* on b strands is a type of diagram of segments (or strands) where all b strands are arranged to start from the bottom of the diagram and move strictly monotonically to the top. See Figure 6. Formally, we can view a braid as the projection of embeddings

$$B : \bigsqcup_{i=1}^{b} I_i \longrightarrow \mathbb{R}^2 \times I,$$

where for each i we have smooth functions $x_i, y_i : I_i \to \mathbb{R}$ such that for $z_i \in I_i$, we have $B(z_i) = (x_i(z_i), y_i(z_i), z_i)$ with $x_i(0) = x_{\sigma(i)}(1) = i$ for some permutation σ, and $y_i(0) = y_i(1) = 0$. We consider braids up to isotopies of such embeddings relative to the boundary of $\bigsqcup I_i$.

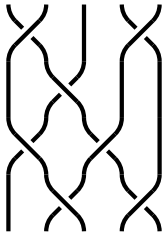

FIGURE 6. **A braid diagram.**

We can arrange the diagram for a braid so that each crossing occurs at a distinct height in the diagram. See Figure 7. Then we can describe braids by elements in a non-commutative group generated by elements σ_i, for $1 \leq i < b$, as shown in Figure 8. This group is called the b-braid group.

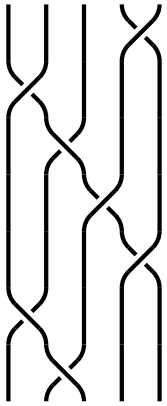

FIGURE 7. **An extended version of the braid diagram from Figure 6**. Each crossing is moved to a different height.

The moves of braid diagrams that do not change the isotopy class of the braid can be encoded as the following relations among the generators:

$$\sigma_i \sigma_{i+1} \sigma_i = \sigma_{i+1} \sigma_i \sigma_{i+1},$$

for $i \leq b-2$, and

$$\sigma_i \sigma_j = \sigma_j \sigma_i$$

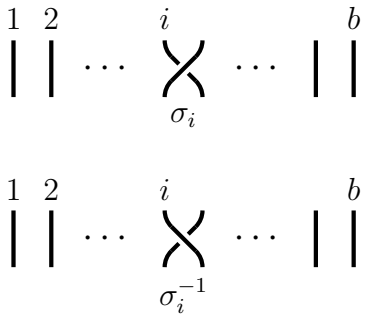

FIGURE 8. **Braid group generators.**

if $|i - j| \geq 2$. See Figure 9. The group element corresponding to a braid is called its *braid word*. We use the convention of writing a braid's generators in the order they appear in the braid diagram from top to bottom.

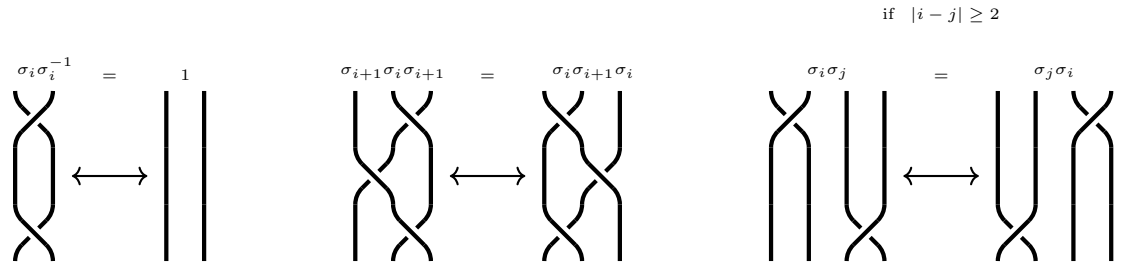

FIGURE 9. **Braid group relations.**

To each braid there is an associated oriented link called its *closure*, which we obtain in the diagram from attaching the top of each segment to the corresponding location at the bottom of the diagram in such a way that we do not introduce new crossings. We take the orientation so that the strands point upward in the braid subset of the diagram. See Figure 10.

Along with the braid group relations, there are two additional moves that preserve the isotopy class of a braid's closure, which all together are called *Markov moves*. The first is *braid conjugation*. If B is a braid word on b strands, then braid

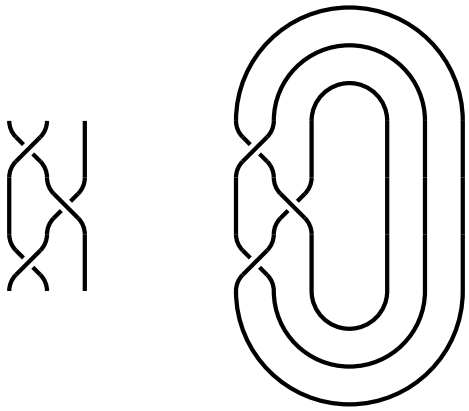

FIGURE 10. **A braid and its closure.**

conjugation is the equivalence

$$B \leftrightarrow \sigma_i B \sigma_i^{-1}$$

for all $1 \leq i < b$. This is equivalent to moving a crossing around the closure from the top to the bottom. See Figure 11. The second additional move is called *stabilization*, which comes in two forms: *positive stabilization* and *negative stabilization*. This is equivalent to a Reidemeister move of type I that is arranged to occur on the rightmost strand of the braid so that an additional strand is added, which is connected to the rest of the braid with either a positive or negative crossing. Stabilization takes a b-braid to a $(b+1)$-braid. We can summarize positive stabilization by

$$B \leftrightarrow B\sigma_b$$

and negative stabilization by

$$B \leftrightarrow B\sigma_b^{-1}.$$

See Figure 12.

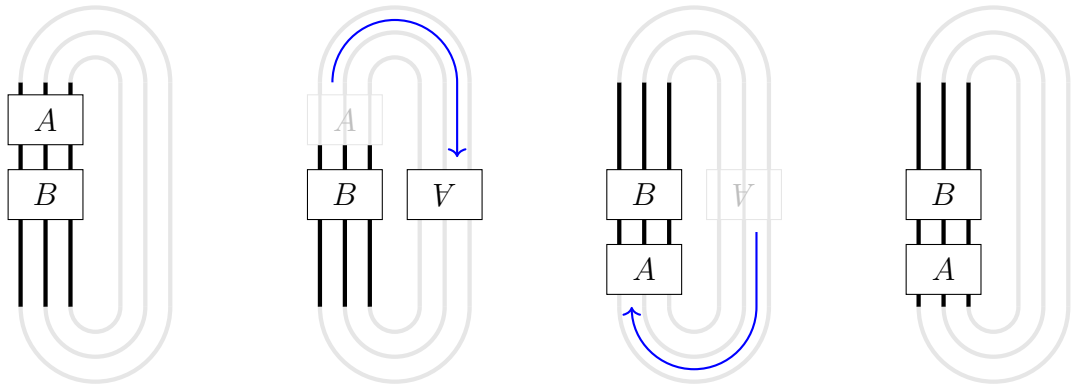

FIGURE 11. **Braid conjugation.**

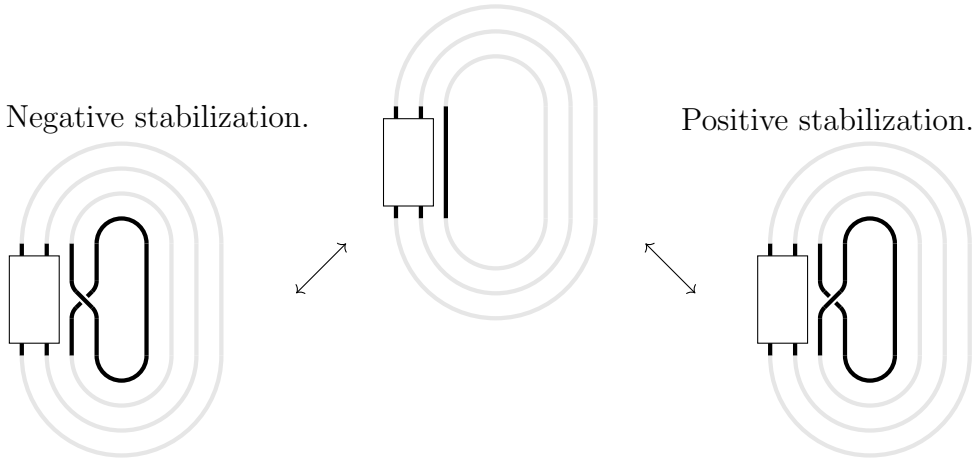

FIGURE 12. **Braid stabilization.**

1.2. Contact Geometry and Transverse Links

A *contact structure* on an odd-dimensional manifold is a hyperplane field in the tangent bundle that is "completely non-integrable." By the Frobenius theorem, we can represent all such hyperplane fields locally by the kernel of a non-degenerate one-form α, and in a $2n+1$-dimensional manifold, the non-integrability condition translates to $\alpha \wedge (d\alpha)^n \neq 0$ everywhere. The standard contact structure on $\mathbb{R}^3$ is defined as the plane field $\ker \alpha$ where $\alpha = dz - y\,dx$. A manifold with a contact structure is called a *contact manifold*.

A typical first-order differential equation

$$F(x, z, z') = 0$$

can be realized as a surface in $\mathbb{R}^3$

$$\{(x, z, y) \in \mathbb{R}^3 \mid F(x, z, y) = 0\}.$$

Given a solution of the differential equation $z(x)$, at each point x with $z = z(x)$, if the slope $y = z'(x)$ is finite, then $dz - y\,dx = 0$. Thus, viewed as a surface in $\mathbb{R}^3$, the solutions of the differential equation are the curves in the surface that are everywhere tangent to the planes $\ker(dz - y\,dx)$. A *contact transformation* is a transformation of $\mathbb{R}^3$,

$$(x, z, y) \mapsto (\hat{x}, \hat{z}, \hat{y})$$

such that there is a nowhere-zero function $\rho : \mathbb{R}^3 \longrightarrow \mathbb{R}$ so that

$$dz - y\,dx = (d\hat{z} - \hat{y}\,d\hat{x})\rho.$$

These are precisely the transformations of $\mathbb{R}^3$ that map the integral curves of F to the transformed differential equation $\hat{F}$. Contact geometry was first studied by Sophus Lie in the form of these contact transformations [Gei01].

The discussion above deals with an ordinary first-order differential equation with unknown function $z : \mathbb{R} \longrightarrow \mathbb{R}$. This generalizes to partial first-order differential equations with unknown function $z : \mathbb{R}^n \longrightarrow \mathbb{R}$ by viewing

$$F(x, z, z') = 0$$

as a hypersurface in $\mathbb{R}^{2n+1}$. Thus, this view of contact structures coming from differential equations can generalize to all odd dimensions. The complete non-integrability condition limits all contact manifolds to odd-dimensional manifolds. In fact, we can view contact manifolds as an odd-dimensional counterpart to symplectic manifolds: manifolds with a closed, non-degenerate 2-form. We can reify this relationship through the construction of symplectic manifolds out of certain nice contact manifolds in which the contact manifold is an embedded hypersurface. Conversely, there are certain symplectic manifolds (X, ω) with hypersurface M,

$$i : M \hookrightarrow X,$$

where (M, ξ) is a contact manifold such that $\xi = \ker \alpha$ and $d\alpha = i^*\omega$ [Etn06, Theorem 5.1]. Such pairs of manifolds often arise when we consider a symplectic manifold coming from an even-dimensional phase space of a mechanical system and an embedded constant-energy hypersurface.

There are many applications of contact geometry in physics: in Hamiltonian mechanics and geometric optics, for example. Their applications have elevated contact manifolds to objects worthy of study in their own right. All closed compact 3-manifolds admit contact structures [Mar71, Théorème 5], though not all admit so-called tight contact structures [EH01, Theorem 1].

A direct way to study contact manifolds is to examine their embedded submanifolds. In the case of hypersurfaces, as we saw earlier, examining the integral curves to the contact structure on the hypersurfaces can be reformulated as a solution to a first-order differential equation. Another important class of submanifolds is curves in the contact manifold. Restricting the curves by the contact structure, we can examine curves that are everywhere tangent to that

structure or curves that are everywhere transverse. It is this latter case that we examine in this dissertation.

A *transverse link* is a link embedded in S^3 that is everywhere transverse to the standard contact structure. Two transverse links are *transversely isotopic* if they are isotopic through a one-parameter family of transverse links. There are two "classical invariants" for transverse knots: the smooth knot type and the self-linking number. In the early 2000s, Etnyre-Honda [EH05, Theorem 1.7] and Birman-Menasco [BM06, Theorem 3] found the first examples of pairs of transverse knots that had the same classical invariants but were not isotopic as transverse knots. Topological knots that have distinct transverse knot representatives with the same classical invariants are called *transversely non-simple*.

Every link can be represented as the closure of some braid, and every braid can be associated to a transverse link; conversely, every transverse link is transversely isotopic to a closed braid [Ben83, Théorèm 8]. The Markov theorem gives conditions under which two braids have closures that are isotopic as links [Mar36, theorem on p. 75]. There is a transverse version of the Markov theorem that gives conditions under which two braids have closures that are isotopic as transverse links [Wri02, Theorem 1] [OS03, theorem on p. 1].

There are now a number of transverse invariants coming from modern techniques in knot theory, particularly gauge theory and holomorphic curves. These include invariants in Heegaard Floer homology [LOSSz09, OSzT08, Kan18], monopole Floer homology [BS18], and knot contact homology [Ng11].

Closely related to these is Khovanov homology [Kho05], a categorization of the Jones polynomial, i.e, its graded Euler characteristic is the Jones polynomial. Khovanov homology is a bigraded abelian group that is computed from the

hypercube of resolutions of a planar diagram of a link. In [Pla06], Plamenevskaya defined an invariant of transverse links as a distinguished element in Khovanov homology. Unlike the invariants above, it is not known to be effective. That is, there is no known pair of transverse links that have the same classical invariants but are distinguished by Plamenevskaya's invariant. Lipshitz, Ng, and Sarkar further studied and refined this invariant and showed it is the same in pairs of transverse links related by negative flypes and pairs related by SZ moves [LNS15, Theorem 4.15].

With $\mathbb{Z}/2$-coefficients, Ozsvath and Szabó constructed a spectral sequence from Khovanov homology to the Heegaard Floer homology group $\widehat{HF}$ of the branched double cover [OSz05, Theorem 1.1]. In attempting to lift this spectral sequence to $\mathbb{Z}$ coefficients, Ozsváth, Rasmussen, and Szabó defined a variant of Khovanov homology, called odd Khovanov homology, and conjectured there is a spectral sequence from it to $\widehat{HF}(\Sigma(K))$ with $\mathbb{Z}$-coefficients [ORSz13, Conjecture 1.9]. In spite of a similar definition, odd Khovanov homology has different properties from even Khovanov homology. The unreduced and reduced odd Khovanov homologies have a simpler relationship than in the even case. Shumakovitch showed there is more torsion in reduced odd Khovanov homology than reduced even Khovanov homology [Shu11, Subsection 3.A]. Although odd Khovanov homology is an effective invariant, it does not distinguish knots related by a Conway mutation [Blo10, Theorem 1]. There is no known analogue of the Lee spectral sequence, an object defined in [Lee03, Lee05] (cf. [Ras10]). This last observation is notable given that there is a close relationship between Plamenevskaya's invariant and the Lee spectral sequence [LNS15, Theorem 4.2].

1.3. The Results

In this paper, we take a diagram D of a transverse link L, and construct an analogue of Plamenevskaya's invariant in odd Khovanov homology, $\psi(D)$.

Theorem 2. *The element $\psi(D) \in Kh'(L)$ is a transverse link invariant, which is well defined up to a sign.*

This theorem is restated more precisely as Theorem 7 in Chapter III. In Proposition 13, we show that the odd Plamenevskaya invariant of the negative stabilization of another transverse link is zero. In Proposition 14, we show that if L' can be obtained from L by replacing a single positive crossing with a 0-smoothing, then the invariants of each are related by the associated homomorphism $Kh'(L) \longrightarrow Kh'(L')$. Unlike even Khovanov homology [Kho06, Theorem 1], it is not known if odd Khovanov homology is natural (cf. [Put10]), so this identification is weaker than the analogous identification in the even case [Pla06, Theorem 4].

1.4. Organization

This paper begins by giving a deeper exposition on transverse links in Section 2.1. In Section 2.2, we define grid diagrams: a useful tool for specifying and studying transversely non-simple knots. We explain the construction of odd Khovanov homology in Section 2.4. The odd analog of Plamenevskaya's invariant is defined in Chapter III, and, using the transverse Markov theorem, we prove it to be invariant in Theorem 7. In Chapter IV, we investigate the reduced odd Khovanov homology. There, we define a reduced version of the invariant, and in Proposition 11, prove that the unreduced invariant can be identified with the reduced invariant via the isomorphism between full odd Khovanov homology

and reduced odd Khovanov homology. In Chapter V, we investigate the odd invariant's properties analogous to those of the even Plamenevskaya invariant. In Chapter VI, we discuss the author's computer program for studying the invariant and observations made using it.

CHAPTER II

BACKGROUND

2.1. Transverse Knots

A *contact structure* on a 3-manifold M is a plane field ξ that is generic at each point. Heuristically, the generic condition means that, locally, there is no surface that is tangent to the plane field at each point of the surface. Since a plane field can be represented locally by the kernel of a 1-form, the generic condition can be specified in terms of the 1-form. Namely, by the Frobenius theorem, if $\xi = \ker \alpha$, then ξ is generic if $\alpha \wedge d\alpha \neq 0$ everywhere.

An important example is the contact structure $(\mathbb{R}^3, \xi_{std})$ defined by $\xi_{std} = \ker \alpha$ where

$$\alpha = dz - y\,dx.$$

See Figure 13.

Two contact structures (M, ξ) and (M, ξ') are *contactomorphic* if there is a diffeomorphism $f : M \longrightarrow M$ such that $f_*(\xi) = \xi'$. Darboux's theorem [Dar82, Section X] states that given any contact structure (M, ξ) and any point $p \in M$, there is a neighborhood N of p, a neighborhood U of $0 \in \mathbb{R}^3$, and a contactomorphism,

$$f : (N, \xi|_N) \longrightarrow (U, \xi_{std}|_U).$$

That is to say, there is nothing interesting in a contact structure locally, as all contact structures look the same near a point.

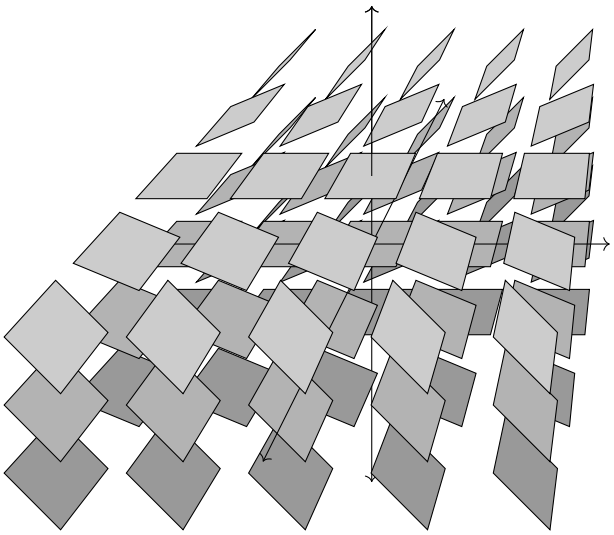

FIGURE 13. **The standard contact structure in $\mathbb{R}^3$.** Given by $\xi_{sym} = \ker(dz - y\,dx)$.

Viewing S^3 as the unit 3-sphere in $\mathbb{R}^4$, we can define a 1-form along S^3,

$$\alpha = (x\,dy - y\,dx + z\,dw - w\,dz)|_{S^3},$$

and define $\xi'_{std} := \ker \alpha$. We can show that, via stereographic projection, $(\mathbb{R}^3, \xi_{std})$ is contactomorphic to

$$(S^3 \backslash \{p\}, \xi'_{std}|_{S^3 \backslash \{p\}}).$$

There is a global contactomorphism $f : (\mathbb{R}^3, \xi_{std}) \longrightarrow (\mathbb{R}^3, \xi_{sym})$, where ξ_{sym} is defined in cylindrical coordinates (r, θ, z) by

$$\xi_{sym} = \ker(dz + r^2\,d\theta).$$

See Figure 14.

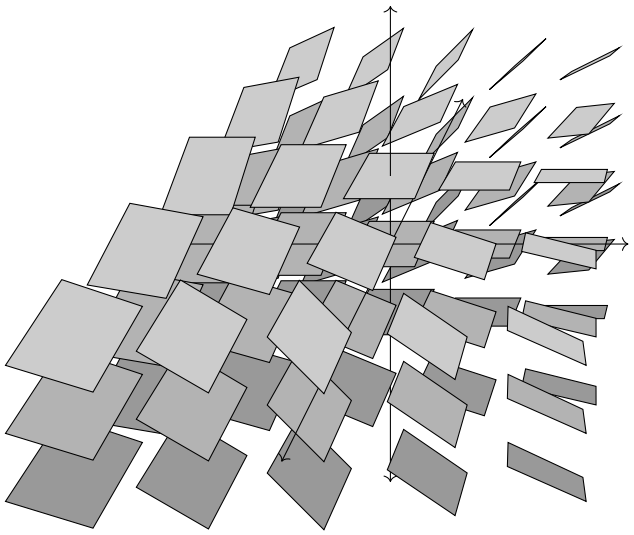

FIGURE 14. **The standard symmetric contact structure in $\mathbb{R}^3$.** Given by $\xi_{sym} = \ker(dz + r^2\, d\theta)$.

A curve, $\gamma : I \longrightarrow M$ in a contact structure (M, ξ) is *transverse* to ξ if at each point p in the curve, we have

$$T_p\gamma \oplus \xi_p = T_pM.$$

A *transverse link* in (M, ξ) is a link whose components are all transverse to ξ when viewed as curves. Without specifying the contact structure, we mean a link that is transverse with respect to $(\mathbb{R}^3, \xi_{std})$ or $(\mathbb{R}^3, \xi_{sym})$. Two transverse links are isotopic if they are isotopic through a family of transverse links.

Theorem 3 (Alexander, [Ale23])**.** *Each topological link is topologically isotopic to the closure of a braid.*

If we take a neighborhood of a circle in the xy-plane with a large enough radius, the contact planes become steep enough so that any braid closure can be transversely embedded in the standard symmetric contact structure. Thus, for each

topological link, we can produce a transverse link. Conversely, every transverse link is transversely isotopic to a braid closure [Ben83, Théorème 8].

Theorem 4 (Markov, [Mar36, Theorem p. 75]). *Two braids B and B' have isotopic closures if and only if they are related by a finite number of the following moves:*

- *braid group relations,*
- *braid conjugation,*
- *positive and negative braid stabilizations and destabilizations.*

"Transversely isotopic" is a refinement of "isotopic," thus it is not surprising that the transverse analog of Theorem 4 permits a reduced number of moves. In particular, it removes negative braid stabilizations and destabilizations from the list of moves that preserve transverse isotopy.

Theorem 5 (Transverse Markov Theorem, Wrinkle and Orevkov-Shevchushin, [Wri02, Theorem 1],[OS03, theorem on p.1]). *Two tranverse links L and L' are transversely isotopic if and only if they are related by a finite number of the following moves:*

- *braid group relations,*
- *braid conjugations,*
- *positive braid stabilizations and destabilizations.*

Throughout this paper, transverse links will be represented by braids, oriented vertically. For example, a right-handed trefoil would be represented as in Figure 15 (left), where it is understood that the diagram stands in for the braid's

closure (right). With this convention, every positive and negative crossing has a fixed representation, with a positive crossing coming from the left strand crossing over the right strand as we travel up the braid, and a negative crossing from the right strand crossing over the left strand, as shown in Figure 16.

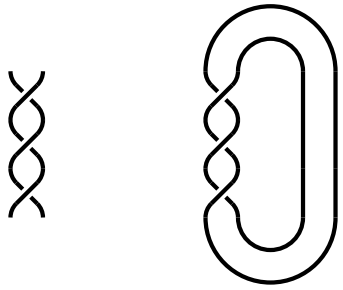

FIGURE 15. **A braid and its closure.**

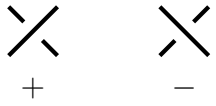

FIGURE 16. **Crossing signs in vertically oriented braids.**

There are two classical invariants of transverse knots: the smooth knot type and the self-linking number. If a transverse knot K has a braid diagram with b strands, n_- negative crossings, and n_+ positive crossings, then its self-linking number is

$$sl(K) = -b + n_+ - n_-.$$

Since the transverse Markov theorem removes negative braid stabilizations from its list of moves between braid diagrams representing the same transverse knot, it is easy to see this is a transverse knot invariant.

A smooth knot type is called *transversely non-simple* if there is more than one transverse representative that has that smooth knot type and each transverse

representative has the same self-linking number. The first transversely non-simple knots were found by [EH05, BM06]. A transverse knot invariant is called *effective* if it can distinguish a pair of different transverse knots with the same smooth knot type and self-linking number.

Just as transverse links are links whose components are everywhere transverse to the standard contact structure, a *Legendrian link* is a link that is everywhere tangent to the standard contact structure. There is a notion of *Legendrian isotopy* analogous to the notion of transverse isotopy. The *front projection* of a Legendrian link is the projection

$$\Pi : (x, y, z) \mapsto (x, z).$$

If we let $\theta \mapsto (x(\theta), y(\theta), z(\theta))$ be the embedding of a Legendrian knot, since it is everywhere tangent to the contact structure, it follows that

$$z'(\theta) - y(\theta)x'(\theta) = 0,$$

and thus

$$y(\theta) = \frac{z'(\theta)}{x'(\theta)}.$$

And so, in the front projection, the slope of the curve corresponds to the value of $y(\theta)$. In particular, given two segments that cross, the segment with a steeper slope is behind the segment with a shallower slope. Example front projections are shown in Figures 17 and 18. Each Legendrian link can be described with such a front projection with the only limitation being that, instead of vertical tangent lines, we have cusps that represent parts of the curve where $x(\theta)$ reaches a local extremum, and thus $x'(\theta) = 0$.

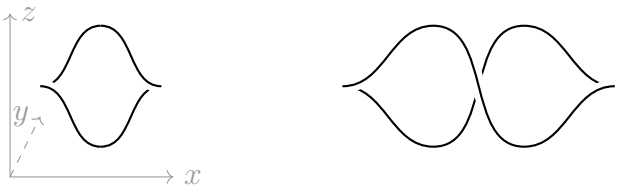

FIGURE 17. **Two Legendrian unknots that are not Legendrian isotopic.**

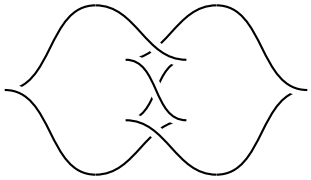

FIGURE 18. **A Legendrian figure-eight knot.**

Legendrian links are useful when studying transverse links because Legendrian links can be specified by their front projection. There is also a set of moves, called the Legendrian Reidemeister moves, which classify front projections of Legendrian links up to Legendrian isotopy. There is not a projection for transverse links that provides an analogous property. Furthermore, there is a well-defined map from Legendrian links to transverse links, called the *positive transverse push off*, which can be specified from the front projection following Figure 19. For a more complete discussion of Legendrian knots, see [Etn05].

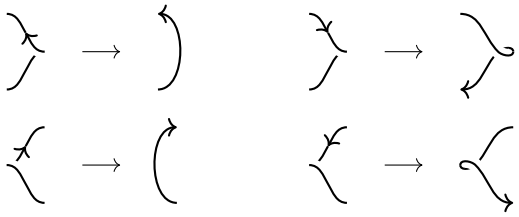

FIGURE 19. **Defining the positive transverse push off of a Legendrian knot.**

2.2. Grid Diagrams

As we have begun to see, there is a rich set of relations between links, braids, transverse links, and Legendrian links. Grid diagrams are a useful tool for making the maps between these sets of equivalence classes well-defined. See Figure 20 (left). A *grid diagram* is an $n \times n$ board or grid on which there is one X and one O in each column and row.

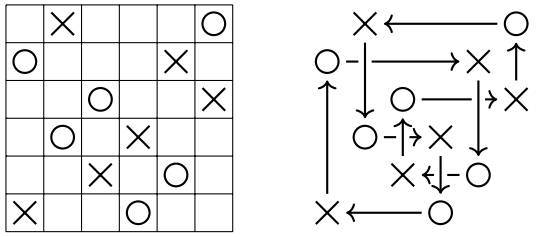

FIGURE 20. **A grid diagram.**

A grid diagram specifies an oriented knot diagram: in each row we connect the X and O in that row with a segment oriented from O to X, and in each column we have a similar segment oriented from X to O. When a vertical segment meets a horizontal segment, the vertical segment crosses over the horizontal one. See Figure 20 (right). This gives us a well-defined map from grid diagrams to links. In this section, we highlight the key points in the relationship between grids and links, braids, Legendrian links, and transverse links. For a more complete discussion, see [NT09].

There is a small set of moves between grid diagrams that preserve the isotopy class of the links they produce. Defining an equivalence relation under these moves, we get a correspondence between equivalence classes of grid diagrams and links. Furthermore, for each oriented link diagram there is a set of grid diagrams that produce isotopic oriented link diagrams. One such grid diagram can be produced

first by twisting each of the crossings so the overpassing segment is vertically oriented. Next, we approximate the segments of the knots with straight segments that are vertical or horizontal. Then, we shift segments as needed so that no two horizontal segments and no two vertical segments are colinear. Finally, we assign each corner in the diagram with an X or an O according to the orientations and use the vertical and horizontal orders to place each corresponding X and O in a grid diagram. See Figure 21.

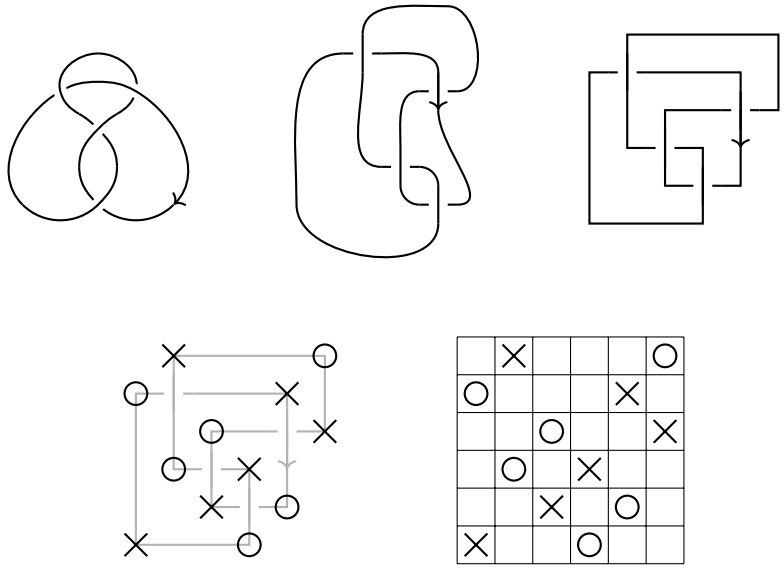

FIGURE 21. **Generating a grid diagram from a knot.**

A grid diagram also can be used to specify a braid. To produce a braid, we start with the link diagram from the grid diagram. Then we take every row in which the X is to the left of the O, and replace the leftward-oriented segment with one coming into the X from the left side, and one coming out of the O to the right side. See Figure 22(b).

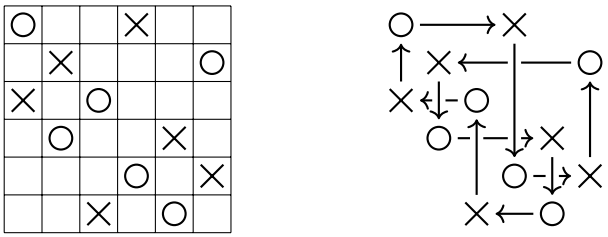

(a) Generating a knot from a grid diagram.

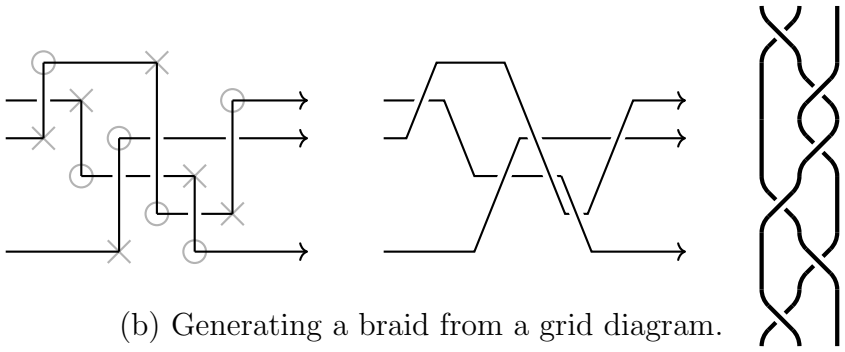

(b) Generating a braid from a grid diagram.

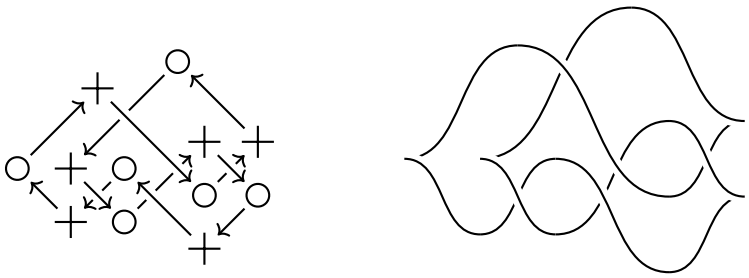

(c) Generating a Legendrian knot from a grid diagram.

FIGURE 22. **Generating knots, Legendrian knots, and braids from grid diagrams.**

Now, every horizontal segment is oriented rightward. If we twist every downward-oriented segment a little counterclockwise, and every upward oriented segment clockwise, the result is a braid.

From each grid diagram, we can produce four braids. The one described above is the rightward braid for the grid diagram, and a similar procedure can also

be adapted to produce upward, leftward, and downward braids. We can restrict the set of grid moves producing isotopic links to one that produces equivalent braids. The restriction depends on the direction of the braid we are producing.

Since for each braid there is a well-defined transverse link, this mapping from grid diagrams to braids gives us a mapping from grid diagrams to transverse links. It is also worth mentioning that if we take the knot diagram from a grid, rotate it clockwise 45 degrees, smooth top and bottom corners, and replace left and right corners with cusps, we can produce a well-defined Legendrian front projection from a grid diagram. See Figure 22(c). There is also a restriction of the set of link-isotopy moves that produces equivalent Legendrian links. Furthermore, it is proven in [KN10, Propositions 3 and 4] that the map from grid diagrams to transverse links via the positive pushoff of a Legendrian knot produces the same transverse link as the map via the rightward braid (the conventions used here match the conventions of [NT09] and are rotated by 90 degrees from the conventions in [KN10]).

Grid diagrams provide a strong tool for studying transversely non-simple knots. They are used in the combinatorial definition of knot Floer homology [MOS09], which was used in [NOT08] to distinguish transversely non-simple pairs. They are also useful because the above process of producing a grid diagram from a knot diagram together with the process of producing a braid from a grid diagram provides a constructive proof of Alexander's theorem (Theorem 3). This is important for us because the definition of the transverse knot invariant central to this dissertation, given in Chapter III, depends on having a braid diagram.

2.3. Cube Complexes

Let $\mathcal{C}$ be a category, and let $\mathcal{I}$ be a finite set. An *$\mathcal{I}$-cube in $\mathcal{C}$* consists of a collection of objects and morphisms of $\mathcal{C}$ as follows. For an $\mathcal{I}$-cube C_*, the *vertices* of the cube are objects corresponding to elements of $\alpha \in \{0,1\}^{\mathcal{I}}$. The *height* of a vertex C_α is defined

$$|\alpha| = \sum_{i \in \mathcal{I}} \alpha(i).$$

The *edges* are morphisms $e_\star : C_{\alpha_0} \longrightarrow C_{\alpha_1}$ where $\alpha_0, \alpha_1 \in \{0,1\}^{\mathcal{I}}$ differ only at a single index $i' \in \mathcal{I}$ with $\alpha_0(i') = 0$ and $\alpha_1(i') = 1$. The *faces* correspond to quadruples $a_{00}, a_{01}, a_{10}, a_{11} \in \{0,1\}^{\mathcal{I}}$ that agree except on a pair of indices, $i_1, i_2 \in \mathcal{I}$ where $a_{jk}(i_1) = j$ and $a_{jk}(i_2) = k$ for $i, j = 0, 1$.

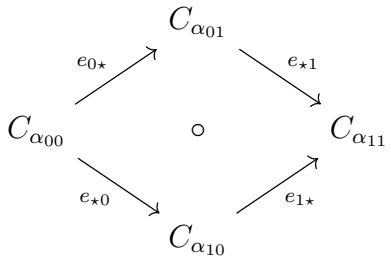

A *commutative $\mathcal{I}$-cube in $\mathcal{C}$* is a $\mathcal{I}$-cube where all faces are required to commute. Thus, with edges labeled as above, faces satisfy $e_{\star 1} \circ e_{0\star} = e_{1\star} \circ e_{\star 0}$. A *skew $\mathcal{I}$-cube in $\mathcal{C}$* where $\mathcal{C}$ is an abelian category is defined similarly, with the condition on faces changed so that all faces are required to anti-commute.

For a (skew) cube C_*, its set of edges is denoted $\mathcal{E}(C_*)$ and for any $\alpha \in \{0,1\}^{\mathcal{I}}$ the subset of edges with C_α as its source is denoted $\mathcal{E}(\alpha)$. Similarly, the set of faces (or squares) is denoted $\mathcal{S}(C_*)$. Note our convention that $\star$ denotes a change from 0 to 1 in the indices of its vertex labels.

A homomorphism between (skew) $\mathcal{I}$-cubes in $\mathcal{C}$ $f_* : C_* \longrightarrow C'_*$, which is called a *(skew) cube map*, consists of a collection of morphisms $f_\alpha : C_\alpha \longrightarrow C'_\alpha$, such that

for each pair of corresponding edges $e[C_*] : C_{\alpha_0} \longrightarrow C_{\alpha_1}$ and $e[C'_*] : C'_{\alpha_0} \longrightarrow C'_{\alpha_1}$, we have

$$f_{\alpha_1} \circ e_\star[C_*] = e_\star[C'_*] \circ f_{\alpha_0}.$$

$\mathcal{I}$-cubes in $\mathcal{C}$ with cube maps form the category of $\mathcal{I}$-cubes $\mathrm{Cube}_{\mathcal{I}}(\mathcal{C})$. Commutative $\mathcal{I}$-cubes in $\mathcal{C}$ with cube maps for the category of $\mathcal{I}$-cubes $\mathrm{CCube}_{\mathcal{I}}(\mathcal{C})$. Skew $\mathcal{I}$-cubes in $\mathcal{C}$ with cube maps form the category of skew $\mathcal{I}$-cubes $\mathrm{SCube}_{\mathcal{I}}(\mathcal{C})$. Note,

$$\mathrm{Cube}_{\emptyset}(\mathcal{C}) \cong \mathrm{SCube}_{\emptyset}(\mathcal{C}) \cong \mathcal{C}.$$

For any abelian category $\mathcal{C}$, $\mathrm{SCube}_{\mathcal{I}}(\mathcal{C})$ is itself an abelian category. For $C_*, D_* \in \mathrm{SCube}_{\mathcal{I}}(\mathcal{C})$, we define

$$E_* = C_* \oplus D_*$$

such that for each $\alpha \in \{0,1\}^{\mathcal{I}}$, we define

$$E_\alpha = C_\alpha \oplus D_\alpha,$$

and for each edge $e : \alpha_0 \longrightarrow \alpha_1$, we define

$$e[E_*] = e[C_*] \oplus e[D_*].$$

Given a skew cube map $f_* : C_* \longrightarrow C'_*$, the mapping cone $\mathrm{Cone}(f_*)$ is a skew $\mathcal{J}$-cube where $\mathcal{J} = \mathcal{I} \sqcup \{\hat{\imath}\}$. Vertices $\alpha \in \{0,1\}^{\mathcal{J}}$ with $\alpha(\hat{\imath}) = 0$ all correspond to the vertices of C_*,

$$\mathrm{Cone}(f_*)_\alpha = C_\alpha$$

with edges between such vertices also coming from C_*. Similarly, vertices with $\alpha(\hat{\imath}) = 1$ all correspond to the vertices of C'_*,

$$\mathrm{Cone}(f_*)_\alpha = C'_\alpha,$$

however the edges between such vertices are the negatives of the edges in C'_*. For edge $e_\star : \alpha_0 \longrightarrow \alpha_1$ with α_0 and α_1 differing only at $\hat{\imath}$, for $\alpha = \alpha_0|_{\mathcal{I}} = \alpha_1|_{\mathcal{I}}$, we have

$$e_\star := f_\alpha.$$

For each $m \in \mathbb{Z}$ there is a functor from skew cubes to (co)chain complexes,

$$\mathrm{Ch}^m : \mathrm{SCube}(\mathcal{C}) \longrightarrow \mathrm{Ch}(\mathcal{C}),$$

where for an object C_* in $\mathrm{SCube}(\mathcal{C})$,

$$\mathrm{Ch}^m(C_*)_r := \bigoplus_{|\alpha|+m=r} C_\alpha,$$

and

$$d^r := \bigoplus_{|\alpha|+m=r, e\in\mathcal{E}(\alpha)} e.$$

For a cube map $f_* : C_* \longrightarrow C'_*$, $\mathrm{Ch}^m(f_*)$ is the chain map g_* where

$$g_r := \bigoplus_{|\alpha|+m=r} f_\alpha.$$

Note, given a skew cube map $f_* : C_* \longrightarrow C'_*$,

$$\mathrm{Ch}^m(\mathrm{Cone}(f_*)) = \mathrm{Cone}(\mathrm{Ch}^m(f_*)).$$

A skew cube map $f_* : C_* \longrightarrow C'_*$ is a *quasi-isomorphism* if $\mathrm{Ch}^m(f_*)$ is a quasi-isomorphism. In skew cubes for which we their associated chain complexes are the prime object of study, we will often use $d^\star$ to denote edges in place of $e_\star$.

2.4. Odd Khovanov Homology

We define $\mathfrak{C}$ to be the subcategory of the $(1 + 1)$-dimensional cobordism category.

Let D be a link diagram and $\mathcal{X}$ be the set of crossings of D. We define $n = |\mathcal{X}|$, and n_- (resp. n_+) as the number of negative (resp. positive) crossings. So, $n = n_- + n_+$. Each crossing has two possible smoothings, which we will label the 0- and 1-smoothings, defined by Figure 23.

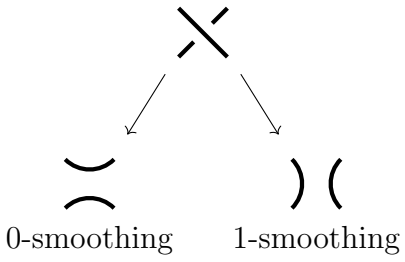

FIGURE 23. **0- and 1-smoothings of a crossing.**

Which is the 0-smoothing and which is the 1-smoothing is independent of the sign of the crossing. However, in the braid representations of a link, the orientation of the crossing immediately makes its sign clear. Thus, for a braid diagram (oriented vertically) we can represent the 0- and 1-smoothings for positive

and negative crossings according to Figure 24. We note that for a positive crossing, the 0-smoothing separates two adjacent strands, whereas the 1-smoothing joins them. On the other hand, for a negative crossing, the 1-smoothing separates adjacent strands, and the 0-smoothing joins them.

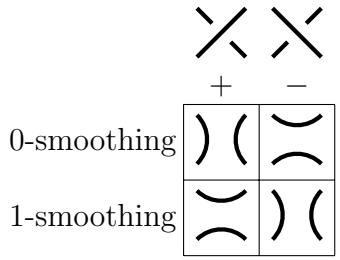

FIGURE 24. **0- and 1-smoothings of a crossing in a vertically oriented braid diagram.**

If each crossing in D is resolved by either a 0- or 1- smoothing, the result is a collection of disjoint circles in the plane, called a *resolution* of D. There is a resolution cube $R(D) \in \mathrm{CCube}_{\mathcal{X}}(\mathfrak{C})$, where the vertex corresponding to each $\alpha \in \{0,1\}^{\mathcal{X}}$ is the resolution obtained by replacing each crossing $x \in \mathcal{X}$ by its $\alpha(x)$-smoothing. The edges correspond to either a merge or a split of a pair of circles as well as the identity cobordism on all other circles.

We describe the elementary cobordisms pictorially with figures where the source of the morphism is the set of circles at the bottom of the figure, and the target is the set of circles at the top. See Figure 25. To preserve the skew structure later, we fix a sign convention by labeling each crossing with an arrow that induces an arrow on the smoothings of this crossing as in Figure 26. There are two possible choices at each crossing.

(a) M: the merge cobordism. (b) S: the split cobordism.

FIGURE 25. **Elementary $(1+1)$-Cobordisms.**

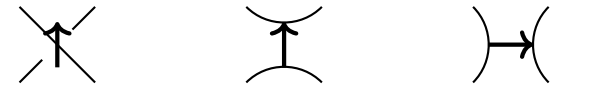

FIGURE 26. **Crossing arrows for orienting the cobordisms in the resolution cube.** The arrows in a single crossing in the knot diagram (left), its 0-smoothing (middle), and its 1-smoothing (right). The arrow in the middle diagram can also be viewed as the 1-handle attached in the cobordism connecting resolutions, which differ by a 0- and 1-smoothing at this crossing.

Each face of the diagram corresponds to one of the four types as depicted in Figure 27. There is a function

$$\mathrm{sgn}_{\mathcal{S}} : \mathcal{S}(R(D)) \longrightarrow \{\pm 1\},$$

where a square is mapped to $+1$ if it is type C or type Y, and -1 if it is type A or type X.

Our construction of the odd Khovanov homology of a link L with diagram D starts with a skew cube $C(D) \in \mathrm{SCube}_{\mathcal{X}}(\mathrm{Mod}_R^{gr})$ where Mod_R^{gr} is the category of graded R-modules. Each vertex module is the exterior algebra on the free R-

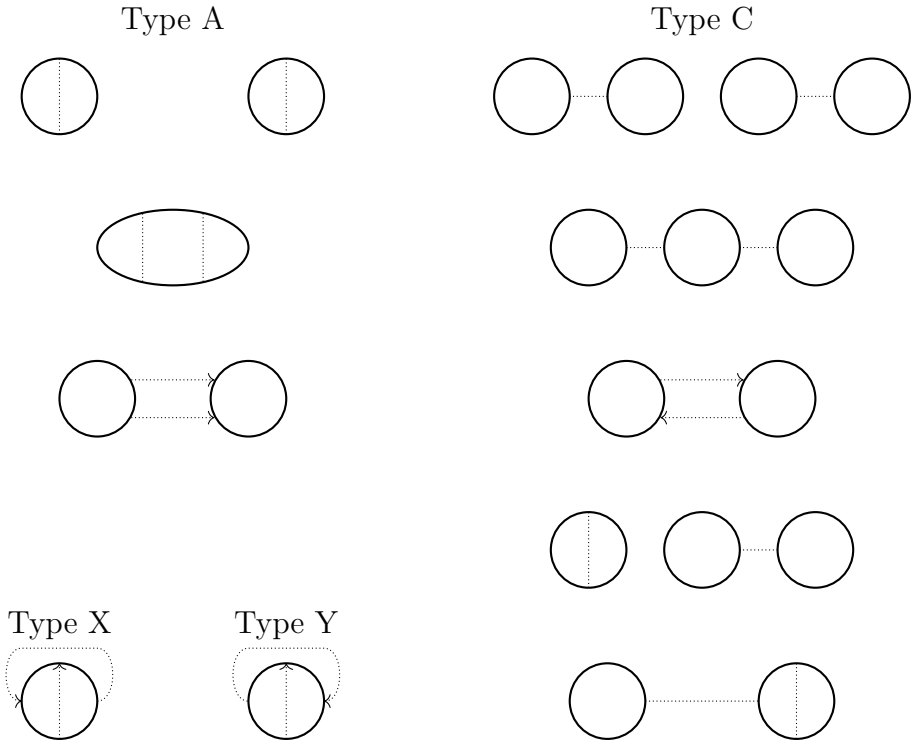

FIGURE 27. **Face types in the resolution cube.** There are four types of faces in the resolution cube depending on the one-handles corresponding to the face's edges. The thicker solid lines represent the relevant circles in the resolution before the cobordisms, and the dotted lines (or arrows) correspond to the one-handles.

module generated by $\{v_1, \ldots, v_k\}$

$$\Lambda^*\langle v_1, \cdots, v_k\rangle$$

where each generator v_i corresponds with a circle a_i in the corresponding vertex of the resolution cube $R(D)$. The construction of the skew cube is inductive on the number of crossings n. At each stage, for a diagram D with n crossings we construct a pair of a skew cube $C(D)$ and a function

$$\mathrm{sgn}_{\mathcal{E}(C(D))} : \mathcal{E}(C(D)) \longrightarrow \{\pm 1\}$$

with the following properties:

1. For a face $C(D)$ of type A or X (resp. C or Y) there are an odd (resp. even) number of edges around the face labeled -1 by $\mathrm{sgn}_{\mathcal{E}(C(D))}$.

2. The maps in the skew cube $C(D)$ are obtained by multiplying the maps from Formulas 2.4.1 and 2.4.2. below by $\mathrm{sgn}_{\mathcal{E}(C(D))}(e)$.

   For the base case $|\mathcal{E}(C(D))| = 1$ we define

$$\mathrm{sgn}_{\mathcal{E}(C(D))}(e) = 1.$$

If the edge e corresponds to the merge cobordism, the corresponding map is defined by

$$v_0, v_1 \mapsto v_0 \sim v_1 \tag{2.4.1}$$

(see Figure 25(a)). If e corresponds to the split cobordism, the map is defined by

$$1 \mapsto (v_0 - v_1) \tag{2.4.2}$$

(see Figure 25(b)) where the arrow in α_0 (as given in Figure 26) points from a_0 to a_1.

In the inductive step, consider a diagram with $n+1$ crossings. Let $\hat{x}$ be one of the crossings, and D_0 and D_1 the diagrams obtained from the 0- and 1-smoothings at $\hat{x}$. By induction, we have a skew cub $C(D_0)$ and a function

$$\mathrm{sgn}_{\mathcal{E}(C(D_0))} : \mathcal{E}(C(D_0)) \longrightarrow \{\pm 1\},$$

satisfying Properties 1 and 2. Let $\hat{C}(D_1)$ be the (not necessarily skew) $\mathcal{X}\backslash\{\hat{x}\}$-cube where the maps on the edges are defined by (2.4.1) if the edge corresponds to a merge cobordism, and (2.4.2) if the edge corresponds to a split cobordism. Note, for a face $S \in \mathcal{S}(\hat{C}(D_1))$, it is type A (according to Figure 26) if the face anti-commutes, type C if it commutes, and type X or Y if it both commutes and anti-commutes (i.e., the composition of two consecutive edges on the face is the zero map). So $\mathrm{sgn}_{\mathcal{E}}$ is motivated by the need for a sign assignment that guarantees that each face $S \in \mathcal{S}(C(D_1))$ is skew. We define the $\mathcal{X}\backslash\{\hat{x}\}$-cube $C(D_1)$ to have the same vertices as $\hat{C}(D_1)$. For each edge $e_1 \in \mathcal{E}(C(D_1))$, there is a corresponding edge $\hat{e}_1 \in \mathcal{E}(\hat{C}(D_1))$ and a corresponding edge $e_0 \in \mathcal{E}(C(D_0))$. The pair e_0 and e_1 correspond to edges in $R(D)$, and there, they specify a unique face $S \in \mathcal{S}(R(D))$. We define

$$e_1 = \mathrm{sgn}_{\mathcal{E}(C(D_0))}(e_0)\,\mathrm{sgn}_{\mathcal{S}}(S)\hat{e}_1.$$

Lemma 1. *Defined as above, $C(D_1)$ is a skew cube.*

Proof. Let $S_1 \in \mathcal{S}(\hat{C}(D_1))$. There is a corresponding face $S_0 \in C(D_0)$, and together, these faces specify a 3-cube in $R(D)$ with S_0 as the top face, S_1 as the bottom face, and an additional four lateral faces. By [ORSz13, Lemma 2.1], this cube has an even number of faces of type A and X. We have two cases. In the first case S_0 and S_1 are either both type A or X, or both type C or Y. Thus, by [ORSz13, Lemma 2.1], there are an even number of lateral faces of type A or X. Therefore, by the sign assignment of S_1, there are an even number of negative signs introduced on the edges of S_1. It follows that the parity of the number of edges that map to -1 in S_0 matches the parity for S_1. Since S_0 is skew, and S_1 is of a matching type, then S_1 is skew too.

In the second case, S_0 and S_1 are not of a matching type. That is, one is of type A or X, and the other is of type C or Y. In this case, there is an odd number of lateral faces of type A or X. If S_0 is type C or Y (and thus S_1 is type A or X), by the sign assignment of S_1, there are an even number of negative signs introduced on the edges of S_1. If S_0 is type A or X (and thus S_1 is type C or Y), by the sign assignment of S_1, there are an odd number of negative signs introduced on the edges of S_1. Therefore, we have the number of negative signs introduced on S_1 to guarantee it is skew. □

We define $f_*^{\hat{x}} : C(D_0) \longrightarrow C(D_1)$ where for $\alpha \in \{0,1\}^{\mathcal{X}\setminus\{\hat{x}\}}$, $f_\alpha^{\hat{x}}$ is defined by (2.4.1) or (2.4.2) if the corresponding edge in $R(D)$ is a merge or a split respectively.

Lemma 2. *Defined as above, $f_*^{\hat{x}}$ is a cube map.*

Proof. Let $e_0 \in \mathcal{E}(C(D_0))$ with corresponding $e_1 \in \mathcal{E}(C(D_1))$

$$e_i : C(D_i)_{\alpha_0} \longrightarrow C(D_i)_{\alpha_1}$$

for $i = 0, 1$. In $R(D)$, there is a unique face S specified by e_0 and e_1. By construction, e_1 has the opposite sign assignment of e_0 if S is type A or X, and the same sign assignment if S is type C or Y. Thus, the definition of $C(D_1)$ guarantees that

$$f_{\alpha_1}^{\hat{x}} \circ e_0 = e_1 \circ f_{\alpha_0}^{\hat{x}}.$$ □

Hence, we define the skew cube

$$C(D) = \mathrm{Cone}(f_*^{\hat{x}}).$$

This gives us the next skew cube in the induction step. It remains to be shown that there is a well-defined sign assignment function at this level.

We define

$$\mathrm{sgn}_{\mathcal{E}(C(D))} : \mathcal{E}(C(D)) \longrightarrow \{\pm 1\}$$

as follows. If e corresponds to an edge $e_0 \in C(D_0)$, then

$$\mathrm{sgn}_{\mathcal{E}(C(D))}(e) = \mathrm{sgn}_{\mathcal{E}(C(D_0))}(e_0).$$

If e corresponds to an edge $e_1 \in C(D_1)$, e_0 is the corresponding edge in $C(D_0)$ and S is the unique square connecting their correspondents in $R(D)$, then

$$\mathrm{sgn}_{\mathcal{E}(C(D))}(e) = -\mathrm{sgn}_{\mathcal{E}(C(D_0))}(e_0)\,\mathrm{sgn}_{\mathcal{S}}(S).$$

Note, the negative sign here corresponds to the negative sign in the mapping cone on edges coming from the target of the cone map. On all other edges e (the edges that connect $C(D_0)$ to $C(D_1)$),

$$\mathrm{sgn}_{\mathcal{E}(C(D))}(e) = 1.$$

Lemma 3. *With* $\mathrm{sgn}_{\mathcal{E}(C(D))}$ *defined as above, for each face* $S \in \mathcal{S}(C(D))$*, S has an even number of edges that map to* -1 *if it is type A or X, and an odd number if it is type C or Y.*

Proof. Since $C(D)$ is the mapping cone of $f_*^{\hat{x}} : C(D_0) \longrightarrow C(D_1)$, where the faces of $C(D_0)$ are already assumed to satisfy this property, and the faces of $C(D_1)$ are constructed to do so, it remains only to look at the faces S which connect an edge

e_0 that came from $C(D_0)$ to the edge e_1 that comes an edge in $C(D_1)$. We note the other two edges—obtained from the mapping cone—each map to $+1$.

In the first case, let S be type A or X. In this case

$$\begin{aligned}\operatorname{sgn}_{\mathcal{E}(C(D_1))}(e_1) &= -\operatorname{sgn}_{\mathcal{E}(C(D_0))}(e_0)\operatorname{sgn}_{\mathcal{S}}(S)\\ &= \operatorname{sgn}_{\mathcal{E}(C(D_0))}(e_0).\end{aligned}$$

Thus, there are exactly zero or two edges that map to -1 in S.

In the second case, let S be type C or Y. Then,

$$\begin{aligned}\operatorname{sgn}_{\mathcal{E}(C(D_1))}(e_1) &= -\operatorname{sgn}_{\mathcal{E}(C(D_0))}(e_0)\operatorname{sgn}_{\mathcal{S}}(S)\\ &= -\operatorname{sgn}_{\mathcal{E}(C(D_0))}(e_0).\end{aligned}$$

Thus, there is exactly one edge that maps to -1 in S. □

Note that the maps are R-module homomorphisms, not R-algebra homomorphisms. That is, even though the vertices in $C(D)$ are exterior algebras, it is not necessarily the case that the image of the morphisms respects the product structure. In particular, $f_\alpha^{\hat{x}}$ corresponding to a split is not an R-algebra homomorphism. This map also has a non-trivial degree with respect to the natural grading on the exterior algebras:

$$f_\alpha^{\hat{x}} : \Lambda^k V \longrightarrow \Lambda^{k+1} V.$$

Thus, to produce a bigraded homology of our chain complex, we will define a quantum grading on the vertex vector spaces with respect to which the edge homomorphisms are homogeneous. The quantum grading Q is defined such that

the grading of $\Lambda^k V_\alpha$ is

$$Q = (\dim V_\alpha) - 2k + n_+ - 2n_- + |\alpha|.$$

We define the odd Khovanov homology, $Kh'(D)$, to be the homology of $\mathrm{Ch}^{-n_-}(C(D))$.

Theorem 6 (Ozsváth-Rasmussen-Szabó, [ORSz13, Theorem 1.3])**.** *If L is a link and D is a diagram of L, then $Kh'(D)$ is independent of choice of diagram.*

Thus, we can write unambiguously $Kh'(L)$ in place of $Kh'(D)$. If we want to specify homogenous elements with respect to the bigrading, we can write $Kh'_{r,q}(L)$.

Even Khovanov homology $Kh(L)$ is defined similarly. It uses a different functor, and is natural in the sense that if there is any cobordism between a pair of links, then there is a morphism that is well defined up to sign between their even Khovanov homologies [Jac04, Theorem 2]. An analogous result has not been proven for odd Khovanov homology, but it is conjectured to be true.

We will often take an abstract diagram, usually called D, and focus on one part of that diagram. That is, a braid diagram will often be restricted so as to not show all of the diagram; there may be additional crossings and strands unseen.

If the highlighted part of the diagram has only one crossing x' we can think of D_0 as the $(\mathcal{X}\backslash\{x'\})$-cube with the 0-smoothing at x'. Likewise, we think of D_1 as the cube with the 1-smoothing at x'.

If the highlighted part of the diagram has more than one crossing, we number the crossings from top to bottom and then use subscripts to denote which smoothings are used in the resolution in the order corresponding to the subscripts. For example, if we highlight two crossings, $x' \in \mathcal{X}$ at the top of the diagram and

$x'' \in \mathcal{X}$ below it, then D_{10} is the $(\mathcal{X}\backslash\{x', x''\})$-cube that has the 1-smoothing at x' and the 0-smoothing at x''. This continues analogously for diagrams with more highlighted crossings.

Likewise, for the skew cube complex $C(D)$, there are related subquotients such as $C(D_{01})$ and $C(D_{11})$. From the large complex, we inherit R-module homomorphisms F_e on each of these edges. In resolutions of highlighted diagrams, this leads to a chain map between them given by the edges between corresponding resolutions. For example, between $C(D_{010})$ and $C(D_{110})$, there is a skew cube map $e_{\star 10} : C(D_{010}) \longrightarrow C(D_{110})$.

We will often abuse notation and use $C(D)$ to refer to both the skew cube complex and the chain complex $\mathrm{Ch}^{-n_-}(C(D))$.

CHAPTER III

THE INVARIANT

3.1. Definition of the Invariant

Definition 1. *Let L be a transverse link and D be a braid diagram of L. In the resolution cube associated to D, let α' be the unique resolution where the braid representation is separated into b parallel bands. This resolution corresponds to the vector space $\Lambda^* V_{\alpha'}$, where $V_{\alpha'} = \langle v_1, \ldots, v_b \rangle$. We define $\psi(D)$ first on the level of the chain complex to be a generator of $\Lambda^b V_{\alpha'}$,*

$$\psi(D) := v_1 \wedge \cdots \wedge v_b.$$

From the braid representation, it is easy to see that this resolution is the one in which there is a 0-smoothing for every positive crossing and a 1-smoothing for every negative crossing.

3.2. The Invariant as Seen in Homology

Proposition 1. *$\psi(D)$ is a cycle.*

Proof. There are two cases. If the resolution corresponding to the vertex in which $\psi(D)$ resides is one with a 1-smoothing at every crossing (that is, every crossing in D is a negative crossing), then the next vector space in the chain complex is the 0 vector space, so the differential from the vector space containing $\psi(D)$ is the zero map. Thus every element of $\Lambda^* V_{\alpha'}$ is trivially a cycle, $\psi(D)$ included.

In the second case, there is at least one 0-smoothing in the corresponding resolution. The differential that maps out of $\Lambda^* V_{\alpha'}$ in this case is a sum of maps,

each corresponding to a merge cobordism, one for each 0-smoothing. This is because at each 0-smoothing, the parallel strings on either side of the smoothing merge into a single circle after becoming the 1-smoothing. See Figure 28. We will show that for any one of these maps $\psi(D)$ is mapped to 0, thus $d(\psi(D)) = 0$ and is therefore a cycle.

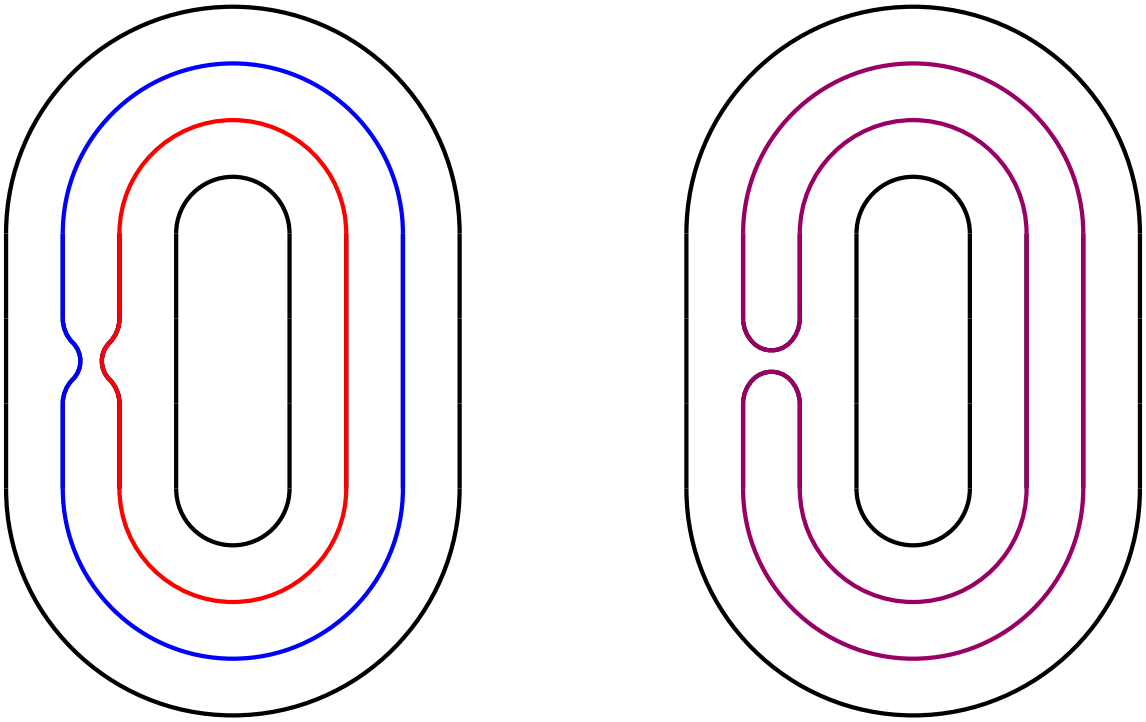

FIGURE 28. **Edge maps out of the invariant's resolution.** The diagrams of the 0-smoothing (left) and 1-smoothing (right) of a single positive braid crossing. The two circles (blue and red) in the 0-smoothing on the left merge into a single circle (purple) on the right.

If the merging components in the diagram are a_{i_0} and a_{i_1}, corresponding to generators v_{i_0} and v_{i_1} resp., the merge map on the vector spaces is induced by the quotient map,

$$q : V_{\alpha'} \longrightarrow V_{\alpha'}/(v_{i_0} - v_{i_1}).$$

The image of the quotient map $V_{\alpha'}/(v_{i_0} - v_{i_1})$ is isomorphic to the vector space generated by the elements corresponding to the components in the target resolution $\langle v_1, \ldots, (v_{i_0} \sim v_{i_1}), \ldots, v_b \rangle$ since there will be one fewer component there after the merge. Since $q(v_{i_0}) = q(v_{i_1})$, then $\tilde{q}(\psi(D)) = 0$ under the induced map because two of the factors in the wedge product map to the same vector. $\square$

Thus, $\psi(D)$ defines an element of homology. We will abuse our notation and refer to both the cycle and its class in homology by $\psi(D)$.

Proposition 2. *The distinguished element $\psi(D)$ is in $Kh'_{0,sl(L)}(L)$.*

Proof. Let $\psi(D)$ be the distinguished element of the homology defined above corresponding to the diagram D. In the chain complex, $\psi(D)$ is an element of $\Lambda^* V_{\alpha'}$ where $V_{\alpha'} = \langle v_1, \ldots, v_b \rangle$ is the vector space with a generator associated to each of the b parallel strands. In particular, the Q grading on $\Lambda^b V_{\alpha'}$ is given by

$$Q = (\dim V_{\alpha'}) - 2b + n_+ - 2n_- + |\alpha'|$$

and because of the choice of α', the number of 1-smoothings is the number of negative crossings in D. Thus, we have $|\alpha'| = n_-$, so

$$\begin{aligned} Q &= -b + n_+ - n_- \\ &= sl(L). \end{aligned}$$

For each resolution α, the homological grading r on V_α is defined such that $|\alpha| = r + n_-$. Thus, since $|\alpha'| = n_-$, then $r = 0$. Therefore, $\psi(D) \in Kh'_{0,sl(L)}(L)$. $\square$

3.3. Invariance

In this section, we will show that $\psi(D)$ is an invariant of transverse links. To do this, we rely upon the transverse Markov theorem—Theorem 5—and show that $\psi(D)$ is invariant under braid group relations and positive braid stabilizations. It is trivially the case that $\psi(D)$ is unchanged by braid conjugations since two braids related by braid conjugation have closures whose diagrams are isotopic in the plane. Thus, their chain complexes are also canonically isomorphic, and that isomorphism clearly identifies $\psi(D)$. Positive braid stabilization and destabilization corresponds to a Reidemeister move of type I that introduces or removes a single positive crossing. We refer to such a move as a transverse type I Reidemeister move, and we prove invariance of $\psi(D)$ under this move in Proposition 3. The braid group moves can be generated from Reidemeister moves of types II and III. We show the invariance of $\psi(D)$ under these moves in Propositions 4 and 5.

Proposition 3. *Let D and $\hat{D}$ be two braid diagrams for a transverse link L related by a single transverse type I Reidemeister move (R1), where $\hat{D}$ is the diagram with the additional positive crossing. There is a quasi-isomorphism $\rho : C(D) \longrightarrow C(\hat{D})$ such that $\rho(\psi(D)) = \psi(\hat{D})$.*

Proof. Let D and $\hat{D}$ be as described above. Focusing on the additional positive crossing, $\hat{D}$ has two associated diagrams, D_0 (resp. D_1) where the 0-smoothing (resp. 1-smoothing) resolves the additional crossing. The resolution cube of D_1 is isotopic to the resolution cube of D at corresponding vertices, thus there is a natural identification of $\psi(D)$ and $\psi(D_1)$. On the other hand, the resolution cube of D_0 is isotopic to the resolution cube of $D \sqcup a_0$. See Figure 29.

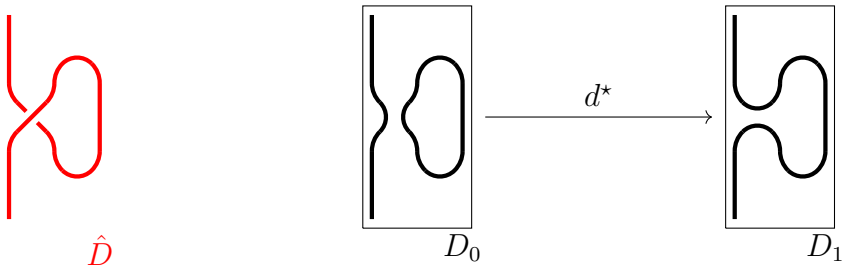

FIGURE 29. **The Resolution Cube for $\hat{D}$: diagram after a transverse RI move.**

In their respective chain complexes, we will use the same generators for equivalent circles. In particular, in each vertex in the resolution cube we will always label the circle to which a_0 attaches as a_1. We associate a_0 to the generator v_0, and a_1 to v_1. We also note, by using the same generators for equivalent circles, since

$$C(D_1) \oplus (v_0 \wedge C(D_1)) \cong C(D) \oplus (v_0 \wedge C(D)) \cong C(D \sqcup a_0) \cong C(D_0),$$

there is a natural inclusion of the first summand, $\imath : C(D_1) \hookrightarrow C(D_0)$. If we define $w : C(D_0) \longrightarrow C(D_0)$ by $w(\omega) = (v_0 - v_1) \wedge \omega$, the composition $w \circ \imath : C(D_1) \longrightarrow C(D_0)$ induces an isomorphism of chain complexes between $C(D_1)$ and $(v_0 - v_1) \wedge C(D_0)$. In particular, if we let b be the braid index of D and thus the braid index of D_1, we have

$$\begin{aligned} w \circ \imath(\psi(D_1)) &= w \circ \imath(v_1 \wedge \cdots \wedge v_b) \\ &= (v_0 - v_1) \wedge (v_1 \wedge \cdots \wedge v_b) \\ &= v_0 \wedge v_1 \wedge \cdots \wedge v_b. \end{aligned}$$

Now, we consider the chain map $d^\star : C(D_0) \longrightarrow C(D_1)$, which is the map induced by the cobordism merging a_0 and a_1. This map is the quotient map given

by the identification of v_0 with v_1. With this setup, the chain complex $C(\hat{D})$ is isomorphic to the mapping cone $\mathrm{Cone}(d^\star)$.

On the chain complex level, $\ker d^\star$ is isomorphic to $(v_0 - v_1) \wedge C(D_0)$. Since $d^\star$ is surjective, it follows that $C(\hat{D}) \cong \mathrm{Cone}(d^\star)$ is quasi-isomorphic to $\ker d^* \cong (v_0 - v_1) \wedge C(D_0)$ via $j : \ker d^\star \hookrightarrow \mathrm{Cone}(d^\star)$. Thus, we have a quasi-isomorphism

$$\bar{\jmath} : (v_0 - v_1) \wedge C(D_0) \cong \ker d^\star \longrightarrow C(\hat{D}),$$

with

$$\bar{\jmath}(v_0 \wedge v_1 \wedge \cdots \wedge v_b) = v_0 \wedge v_1 \wedge \cdots \wedge v_b = \psi(\hat{D}).$$

Letting $\rho : C(D) \longrightarrow C(\hat{D})$ be the composition $\bar{\jmath}$ after $w \circ \imath$, it follows that ρ is a quasi-isomorphism such that

$$\rho(\psi(D)) = \psi(\hat{D}). \qquad \square$$

Proposition 4. *Let D and $\hat{D}$ be two braid diagrams of a transverse link L related by a single type II Reidemeister move (R2), where D is the diagram with more crossings. There is a quasi-isomorphism $\rho : C(D) \longrightarrow C(\hat{D})$ such that $\rho(\psi(D)) = \psi(\hat{D})$.*

Proof. Let D and $\hat{D}$ be as described above. The resolution cube for D is illustrated in Figure 30. We note $C(D)$ can be represented by the diagram below as a mapping cone of a map between two mapping cones.

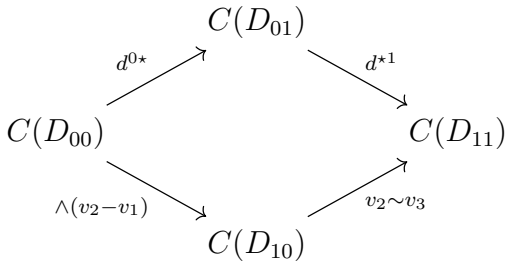

By the arrangement in Figure 30, it follows that $\psi(D) \in C(D_{01})$.

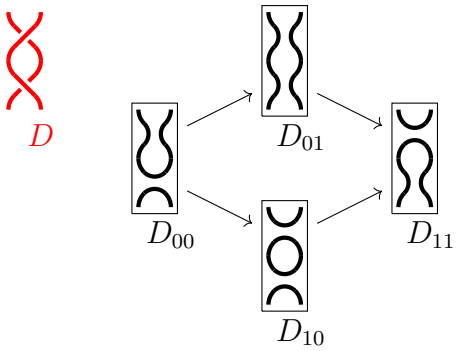

FIGURE 30. **The resolution cube for D: the diagram after an RII move.**

We let $X \subset C(D_{10})$ be the kernel of the contraction with v_2^*, the dual of the generator associated to the disjoint circle in D_{10}. Note, since X and $C(D_{11})$ are isomorphic via the quotient map $v_2 \sim v_3$, it follows that the subquotient complex corresponding to the isomorphism's mapping cone $A =$

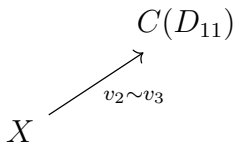

is acyclic. Thus, $C(D)/A$, represented in the diagram below, is quasi-isomorphic to $C(D)$.

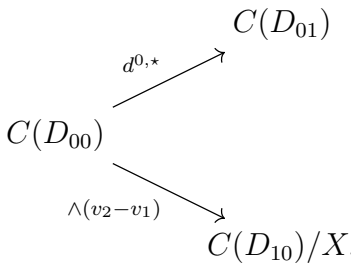

Let $q : C(D) \longrightarrow C(D)/A$ be that quotient map, which is a quasi-isomorphism. Since $\psi(D) \in C(D_{01})$ is the sole representative in its equivalence class in the quotient, then $q(\psi(D)) = \psi(D)$. Furthermore, since $C(D_{00})$ and $C(D_{10})/X$ are isomorphic under the map generated from $1 \mapsto (v_1 - v_2)$, then $(C(D)/A)/C(D_{01})$ is acyclic. Thus $C(D_{01})$ is quasi-isomorphic to $C(D)/A$, and the map is the natural inclusion map. Under this map, we have that $\psi(D) \in C(D_{01}) \subset C(D)$ is unchanged. Finally, since there is a trivial isomorphism between $C(\hat{D})$ and $C(D_{01})$, it follows that $\psi(\hat{D}) = \rho(\psi(D))$, where ρ is the quasi-isomorphism between $C(D)$ and $C(\hat{D})$ obtained from the compositions of the quotient maps above and the trivial isomorphism from $C(D_{01})$ to $C(\hat{D})$. □

Proposition 5. *Let D and $\hat{D}$ be two braid diagrams of a transverse link L related by a single type III Reidemeister move (R3). There is a chain complex C and quasi-isomorphisms,*

$$\rho : C(D) \longrightarrow C \qquad \textit{and} \qquad \hat{\rho} : C(\hat{D}) \longrightarrow C,$$

such that $\rho(\psi(D)) = \hat{\rho}(\psi(\hat{D}))$.

Proof. Let D and $\hat{D}$ be two link diagrams that are related by a single Reidemeister move of type 3, (R3). Focusing on the three crossings involved in the (R3) move, we can represent $C(D)$ via the cube depicted in Figure 31. From the blue map in

Figure 31

$$d^{0\star 0} : C(D_{000}) \longrightarrow C(D_{010})$$

we define

$$\tilde{d}^{0\star 0} : \omega \mapsto d^{0\star 0}(\omega) \wedge v_0,$$

where v_0 is the generator associated to the sole circle entirely shown in D_{010}. Thus, if we denote the complex from the mapping cone of $\tilde{d}^{0\star 0} : C(D_{000}) \longrightarrow C(D_{010}) \wedge v_0$ by $C(\tilde{D}_{0\star 0})$, it follows that there is a quasi-isomorphism between $C(D)$ and $C(D)/C(\tilde{D}_{0\star 0})$. We also note that this quasi-isomorphism is the identity map on parts of the cube uninvolved in the quotient, namely on $C(D_{111})$.

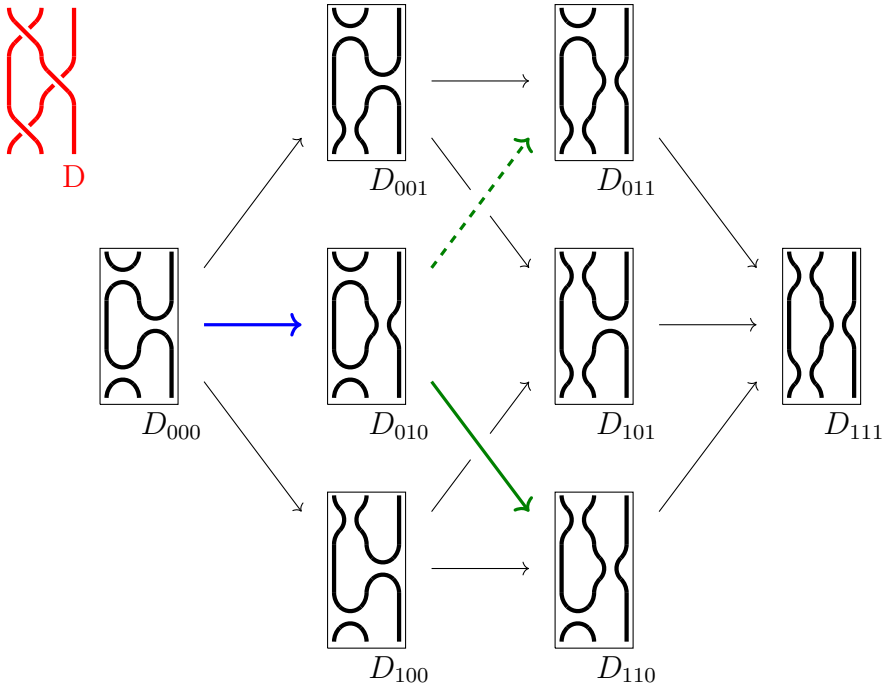

FIGURE 31. **The resolution cube for D: the diagram before an RIII move.**

We define $\mathring{C}$ to be the complex from the mapping cone of the identification of $C(D_{010})/v_0$ with $C(D_{011}) \cong C(D_{110})$, shown in Figure 32. Since the map is an

isomorphism, this complex is acyclic. It can be identified with either green arrow in $C(D)$ in Figure 31. There is a chain map $\Psi : \mathring{C} \longrightarrow C(D)/C(\tilde{D}_{0\star 0})$, given by the identification of $C(D_{010})/v_0$ in $\mathring{C}$ with $C(D_{010})/(C(D_{010}) \wedge v_0)$ in $C(D)/C(\tilde{D}_{0\star 0})$, and the map from the codomain in $\mathring{C}$ to the quotient via the diagonal identification of $C(D_{011})$ and $C(D_{110})$.

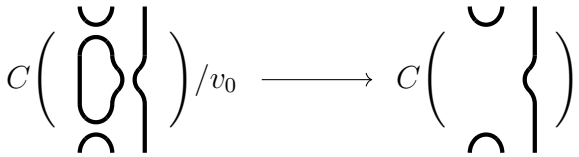

FIGURE 32. **The resolution cube for $\mathring{C}$.**

There is a further chain map Φ from $C(D)/C(\tilde{D}_{0\star 0})$ to the complex from the diagram in Figure 33, which we call C. Up to signs, this map is given by identifying $C(D_{001})$ with $C(A)$, $C(D_{100})$ with $C(B)$, $C(D_{011})$ and $C(D_{110})$ with $C(\Gamma)$, $C(D_{111})$ with $C(\Delta)$, and the map from $C(D_{010})$ being trivial. It is important to note that these signs can be arranged so that they do not impact the mapping between $C(D_{111})$ and $C(E)$ or adjacent maps. So defined, these chain maps form a short exact sequence,

$$0 \longrightarrow \mathring{C} \xrightarrow{\Psi} C(D)/C(\tilde{D}_{0\star 0}) \xrightarrow{\Phi} C \longrightarrow 0.$$

Since $\mathring{C}$ is acyclic, Φ is a quasi-isomorphism. Furthermore, we note that Φ is the identity on $C(D_{111})$. Thus, there is a quasi-isomorphism $\rho : C(D) \longrightarrow C$, which is the identity when restricted to $C(D_{111})$.

For clarity, we simplify the diagram of C to the diagram in Figure 34. This will make the identification of C with the contracted version of $C(\hat{D})$ more visually obvious.

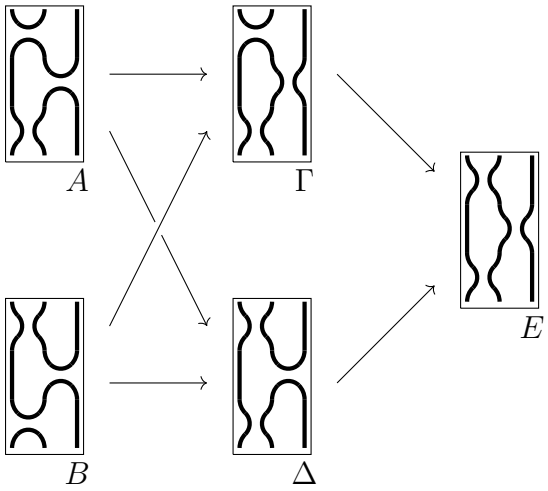

FIGURE 33. **The resolution complex for C: the reduced resolution complex of D.**

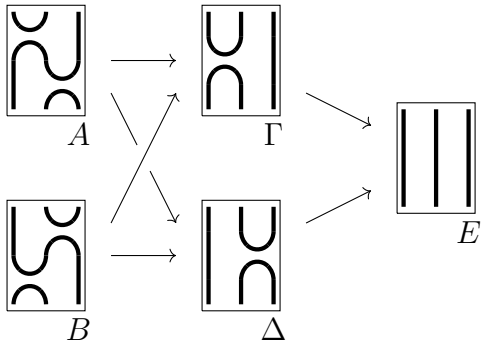

FIGURE 34. **A simplified presentation of D^0: the reduced resolution complex of D.**

In the diagram for $C(D)$, we can think of C as the contraction of the two thick edges. This works because $C(D_{000}) \cong C(D_{110})$ ($\cong C(D_{011})$), and $C(D_{010})$ comes from D_{010}, which is $D_{000} \sqcup O$.

Now, we represent $C(\hat{D})$ by the diagram in Figure 35. Note, like with $C(D)$, we have $C(\hat{D}_{000}) \cong C(\hat{D}_{110}) \cong C(\hat{D}_{011})$, and $C(\hat{D}_{010})$ comes from $\hat{D}_{010}$, which is $\hat{D}_{000} \sqcup O$. Thus, just as with $C(D)$, we can contract the two thick edges in the diagram, giving us $\hat{C}$.

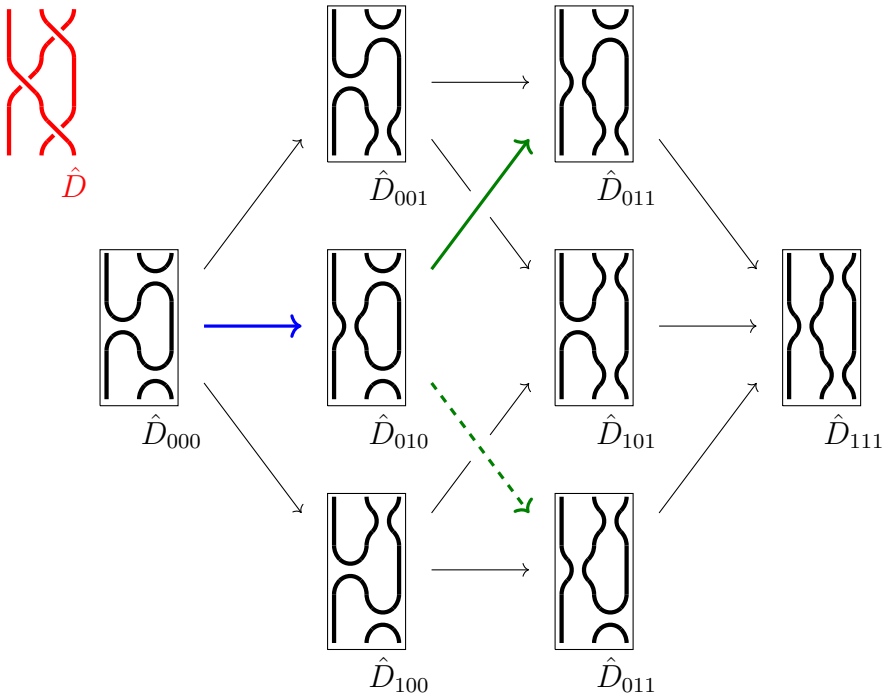

FIGURE 35. **The resolution cube for $\hat{D}$: the diagram after an RIII move.**

The contracted diagram is given in Figure 36 and labeled according to how vertices will correspond with C.

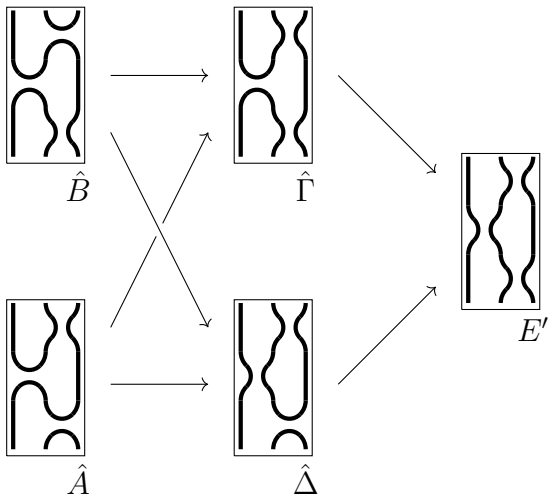

FIGURE 36. **The resolution complex of the contracted version of $\hat{D}$.**

These relations give us a quasi-isomorphism $\hat{\rho} : C(\hat{D}) \longrightarrow \hat{C}$ and as before, the quasi-isomorphism is the identity on $C(\hat{D}_{111})$. The simplified diagram for $C(\hat{D}^1)$ is presented in Figure 37. We note that, except for swapping the position of the leftmost nodes, this corresponds exactly with the simplified diagram of C, thus, $C \cong \hat{C}$. □

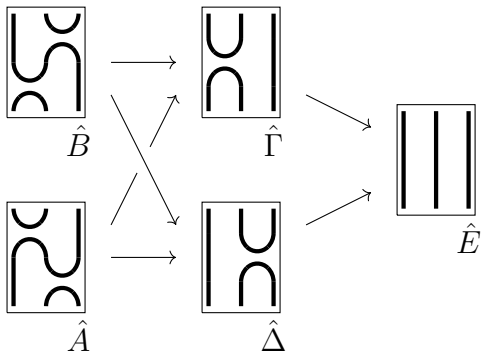

FIGURE 37. **A simplified presentation of the resolution complex for the contracted version of $\hat{D}$.**

Since the chain complexes are bounded, having proved Propositions 3-5, by Theorem 5, we have a more precise formulation of Theorem 2 from Chapter I below.

Theorem 7. *Given two diagrams D and D' of the same transverse link L, there is an isomorphism $\rho : Kh'(D) \longrightarrow Kh'(D')$ such that $\psi(D') = \rho(\psi(D))$.*

Hence, we can unambiguously write $\psi(L)$ instead of $\psi(D)$.

Since $Kh'(L)$ is not known to be natural, $Kh'(L)$ is only (currently) known to be well-defined up to automorphism. Above, we have shown that there is a well-defined map ρ that takes $\psi(D)$ to $\pm\psi(D')$ associated to any sequence of transverse Markov moves from D to D'. In particular, whether $\psi(D)$ vanishes, whether $\psi(D)$

is n-torsion, or whether $\psi(D)$ is divisible by n are all well-defined invariants of the transverse link type.

CHAPTER IV

REDUCED HOMOLOGY

In this chapter, we examine the invariant $\psi(L)$ in the reduced homology. In Section 4.1, we define the groups of the chain complex for the reduced homology $\overline{C}(D)$ as first defined in [ORSz13, Section 4]. The relationship between this chain complex and the full chain complex of odd Khovanov homology is stated in Proposition 7, and is extended to their homologies in Corollary 2. In Section 4.2, we define the differential for this chain complex.

There is a simple relationship between the full and reduced odd Khovanov homologies, and in Section 4.3 we will see conditions that restrict the image of the invariant under this relationship. This restriction yields Corollary 3, which relates to the minimality of a transverse knot. (A related result is given in Chapter V as Proposition 13.)

In Section 4.4, we define a reduced version of the odd Plamenevskaya invariant, a class in the reduced homology $\overline{\psi}(D) \in \overline{Kh'}(L)$. With our maps defined explicitly, it will be possible to identify $\psi(D)$ in the full homology with the reduced version of the invariant under the relationship between the full and reduced homologies, which we state precisely in Proposition 11. From this, it follows that $\overline{\psi}(D)$ is a transverse link invariant, stated as Corollary 5. Thus, we can unambiguously write $\overline{\psi}(L)$.

4.1. The Reduced Chain Complex

The reduced odd Khovanov homology is defined first on the level of complexes of a link diagram D. There are two definitions for the reduced chain complex:

a base-point-dependent definition, and an independent definition. They are isomorphic, and the base-point-dependent definition is useful for proving properties of the reduced odd Khovanov homology. For the base-point-dependent one, we take a point, $p \in D$ not at one of the crossings. In each resolution, this point will belong to a particular circle. Choose labelings of the circles so that in every resolution this circle is labelled a_p, and define

$$\overline{C}^{(p)}(D) = v_p \wedge C(D) \subset C(D).$$

As a consequence of Proposition 8, we will see for $p, q \in D$, that $\overline{C}^{(p)}(D) \cong \overline{C}^{(q)}(D)$.

The base-point-independent definition comes from the exterior algebras $\Lambda^* V_\alpha$ that make up the direct sum that defines $C(D)$. For each resolution α with $V_\alpha = \langle v_1, \ldots, v_n \rangle$, we define $\varphi_\alpha : V_\alpha \longrightarrow R$ by

$$\varphi_\alpha : \sum r^i v_i \mapsto \sum r^i.$$

We define $\Lambda^*_\circ V_\alpha$ to be the subalgebra generated by the kernel of φ_α. That is, $\Lambda^*_\circ V_\alpha = \Lambda^*(\ker \varphi_\alpha)$. Then, we define $\overline{C}(D)$ to be the subcomplex of $C(D)$ corresponding to sum of all $\Lambda^*_\circ V_\alpha$. That this is a subcomplex is a consequence of the following proposition.

Proposition 6. *For each r, $d(\overline{C}^r(D)) \subset \overline{C}^{r+1}(D)$. That is, $\overline{C}(D)$ is a subcomplex of $C(D)$.*

Recall that an edge e in the $\mathcal{X}$-cube of resolutions corresponds to a pair of resolutions, α_0, α_1, which differ at a single crossing x such that $\alpha_0(x) = 0$ and

$\alpha_1(x) = 1$. In the cube of R-modules, we have a map

$$F_e : \Lambda^* V_{\alpha_0} \longrightarrow \Lambda^* V_{\alpha_1}.$$

To prove Proposition 6, we will show for any such edge e,

$$F_e(\Lambda^*_\circ V_{\alpha_0}) \subset \Lambda^*_\circ V_{\alpha_1}.$$

Proposition 6 follows immediately. The proof that the $F_e(\Lambda^*_\circ V_{\alpha_0}) \subset \Lambda^*_\circ V_{\alpha_1}$ is given in parts as the lemmas in Section 4.2.

Proposition 7. *There is an isomorphism*

$$C(D) \cong \overline{C}(D) \oplus \overline{C}(D).$$

4.2. The Induced Differential

Lemma 4. *Let V and W be free R-modules with bases $\{v_i\}$ and $\{w_j\}$. Suppose $T : V \longrightarrow W$ is given by $T(v_i) = \sum_j A_i^j w_j$, and for all i,*

$$\sum_{j=0}^{m} A_i^j = 1.$$

Then the map induced on the exterior algebras

$$\hat{T} : \Lambda^* V \longrightarrow \Lambda^* W,$$

satisfies

$$\hat{T}(\Lambda^*_\circ V) \subset \Lambda^*_\circ W.$$

Proof. Let $\varphi_V : V \longrightarrow R$, be the map given by

$$\sum r^i v_i \mapsto \sum r^i,$$

and $\varphi_W : W \longrightarrow R$ by

$$\sum r^i w_i \mapsto \sum r^i.$$

Thus, $\Lambda^*_\circ V = \Lambda^* \ker \varphi_V$, and $\Lambda^*_\circ W = \Lambda^* \ker \varphi_W$. It suffices to show $T(\ker \varphi_V) \subset \ker \varphi_W$. Let $v = \sum r^i v_i \in \ker \varphi_V$. Then

$$\begin{aligned} T(v) &= \sum_i r^i T(v_i) \\ &= \sum_i r^i \sum_j A_i^j w_j \\ &= \sum_j \left(\sum_i r^i A_i^j \right) w_j. \end{aligned}$$

Therefore,

$$\begin{aligned} \varphi_W(T(v)) &= \sum_j \left(\sum_i r^i A_i^j \right) \\ &= \sum_i r^i \left(\sum_j A_i^j \right). \end{aligned}$$

The internal summand is 1 by our assumption on T, thus

$$\varphi_W(T(v)) = \sum_i r^i.$$

Since $v = \sum r^i v_i \in \ker \varphi_V$, then

$$\varphi_W(T(v)) = 0. \qquad \square$$

Corollary 1. *Let W be a cobordism between disjoint collections of circles α_0 and α_1 entirely made up from a disjoint union of any combination of: the identity cobordism, I; or the merge cobordism, M. Then*

$$F_W(\Lambda^*_\circ V_{\alpha_0}) \subset \Lambda^*_\circ V_{\alpha_1}.$$

Lemma 5. *Let S be the split cobordism (possibly with the identity cobordism on other components) between α_0 and α_1. Then*

$$F_S(\Lambda^*_\circ V_{\alpha_0}) \subset \Lambda^*_\circ V_{\alpha_1}.$$

Proof. We can label the circles of α_0 and α_1 so that $F_S(\omega) = (v_0 - v_1) \wedge \omega$. Since $(v_0 - v_1) \in \ker \varphi_{\alpha_1}$, it follows that if $\omega \in \Lambda^*_\circ V_{\alpha_0}$, then $F_S(\omega) \in \Lambda^*_\circ V_{\alpha_1}$. $\square$

Thus, it follows that $\overline{C}(D)$ is a chain subcomplex of $C(D)$.

Proposition 8. *For any $p \in D$, there is an isomorphism*

$$X^p_D : \overline{C}^{(p)}(D) \longrightarrow \overline{C}(D).$$

Proof. We first define the map on the level of exterior algebras corresponding to resolutions α. Without loss of generality, we take a labeling of D so that in the resolutions $p \in a_0$.

Thus, we will define

$$\chi_D^p : v_0 \wedge \Lambda^* V_\alpha \longrightarrow \Lambda^*_\circ V_\alpha = \Lambda^* \ker \varphi_\alpha.$$

If $V = \langle v_0, \cdots, v_n \rangle$, then we define

$$\hat{V} := \langle v_1, \cdots, v_n \rangle.$$

We will show $\chi_D^p = \theta_2 \circ \theta_1$ where

$$\theta_1 : v_0 \wedge \Lambda^* V_\alpha \longrightarrow \Lambda^* \hat{V}$$

and

$$\theta_2 : \Lambda^* \hat{V} \longrightarrow \Lambda^*_\circ V_\alpha.$$

Every element of $v_0 \wedge \Lambda^* V_\alpha$ can be expressed as $v_0 \wedge \omega$ for $\omega \in \Lambda^* \hat{V}$. So, define θ_1 to be

$$v_0 \wedge \omega \mapsto \omega.$$

Next, we observe that there is a basis of $\ker \varphi_\alpha$,

$$\ker \varphi_\alpha = \langle v_0 - v_i \,|\, 1 \leq i \leq n \rangle.$$

We define θ_2 on the generators of $\Lambda^* \hat{V}$, by

$$v_i \mapsto v_0 - v_i$$

for $1 \leq i \leq n$. This induces an isomorphism of exterior algebras.

Thus, $\chi_D^P = \theta_2 \circ \theta_1$ is an isomorphism of exterior algebras. This extends to a map

$$X_D^p : \overline{C}^{(p)} \longrightarrow \overline{C}(D),$$

which is an isomorphism on the modules of each homological degree. It remains to be shown that X_D^p is a chain map.

It suffices to show that for a map $\tilde{d}$ corresponding to any edge in the cube of exterior algebras,

$$\tilde{d} : \Lambda^* V_{\alpha_0} \longrightarrow \Lambda^* V_{\alpha_1},$$

the following diagram commutes.

$$\begin{array}{ccc} v_0 \wedge \Lambda^* V_{\alpha_0} & \xrightarrow{\tilde{d}} & v_0 \wedge \Lambda^* V_{\alpha_1} \\ \downarrow{\scriptstyle \chi_D^p} & & \downarrow{\scriptstyle \chi_D^p} \\ \Lambda_\circ^* V_{\alpha_0} & \xrightarrow[\tilde{d}]{} & \Lambda_\circ^* V_{\alpha_1} \end{array}$$

If the edge corresponds to a split cobordism, then we have

$$\tilde{d} : \Lambda^* V_{\alpha_0} \longrightarrow \Lambda^* V_{\alpha_1}.$$

Since the split introduces exactly one additional circle, we label the circles so that

$$V_{\alpha_1} = V_{\alpha_0} \oplus \langle v_{n+1} \rangle = \langle v_0, \ldots, v_{n+1} \rangle,$$

and that one of the circles from the split is a_{n+1}. Appropriately restricted, $\tilde{d}$ defines maps on $\Lambda_\circ^* V_\alpha$ and $v_0 \wedge \Lambda^* V_\alpha$ as well. Thus, we have $\tilde{d}(\eta) = (v_i - v_{n+1}) \wedge \eta$, where a_i is the circle that splits.

First, we take the case where $i = 0$.

$$\begin{aligned}\chi_D^p \circ \tilde{d}(v_0 \wedge \omega) &= \chi_D^p((v_0 - v_{n+1}) \wedge v_0 \wedge \omega) \\ &= \chi_D^p(v_0 \wedge v_{n+1} \wedge \omega) \\ &= (v_0 - v_{n+1}) \wedge \theta_2(\omega) \\ &= \tilde{d}\theta_2(\omega) \\ &= \tilde{d} \circ \chi_D^p(v_0 \wedge \omega).\end{aligned}$$

Then we look at the case where $1 \leq i \leq n$.

$$\begin{aligned}\chi_D^p \circ \tilde{d}(v_0 \wedge \omega) &= \chi_D^p((v_i - v_{n+1}) \wedge v_0 \wedge \omega) \\ &= \chi_D^p(v_0 \wedge v_{n+1} \wedge \omega - v_0 \wedge v_i \wedge \omega) \\ &= (v_0 - v_{n+1}) \wedge \theta_2(\omega) - (v_0 - v_i) \wedge \theta_2(\omega) \\ &= (v_i - v_{n+1}) \wedge \theta_2(\omega) \\ &= \tilde{d}(\theta_2(\omega)) \\ &= \tilde{d} \circ \chi_D^p(v_0 \wedge \omega).\end{aligned}$$

Now, we turn our attention to when the edge corresponds to a merge cobordism. Since there is one fewer circle in a resolution after a merge cobordism, if

$$\tilde{d} : \Lambda^* V_{\alpha_0} \longrightarrow \Lambda^* V_{\alpha_1},$$

then we label our circles so that

$$V_{\alpha_0} = V_{\alpha_1} \oplus \langle v_{n+1} \rangle = \langle v_0, \ldots, v_{n+1} \rangle,$$

and v_{n+1} is one of the two circles involved in the merge. Note, this means that if v_j and v_{n+1} are merged by the cobordism, then

$$v_j, v_{n+1} \mapsto v_j$$

and for $1 \leq i \leq n, i \neq j, v_i \mapsto v_i$. This implies, regardless of whether $j = 0$ or not, that

$$\tilde{d}(v_0 \wedge \omega) = v_0 \wedge \tilde{d}\omega.$$

In the merge case, both θ_2 and $\tilde{d}$ are defined on the generators, so if they commute on their generators it follows that they commute on the full exterior algebras.

If $1 \leq i \leq n$,

$$\theta_2 \circ \tilde{d}(v_i) = \theta_2(v_i) = (v_0 - v_i) = \tilde{d}(v_0 - v_i) = \tilde{d} \circ \theta_2(v_i).$$

If $i = n + 1$,

$$\theta_2 \circ \tilde{d}(v_{n+1}) = \theta_2(v_j) = (v_0 - v_j) = \tilde{d}(v_0 - v_{n+1}) = \tilde{d} \circ \theta_2(v_{n+1}).$$

Thus, for all $\omega \in \Lambda^*\langle v_1, \cdots, v_{n+1}\rangle$,

$$\theta_2 \circ \tilde{d}(\omega) = \tilde{d} \circ \theta_2(\omega).$$

This completes the proof. □

Definition 2. *The reduced odd Khovanov homology $\overline{Kh'}(L)$ is defined to be the homology of $\overline{C}(D)$.*

Corollary 2 (Ozsváth-Rasmussen-Szabó, [ORSz13, Proposition 1.7])**.**

$$Kh'_{m,s}(L) = \overline{Kh'}_{m,s-1}(L) \oplus \overline{Kh'}_{m,s+1}(L).$$

In Section 4.4, we define $\overline{\psi}(D)$ and prove it to be invariant, and we identify it with $\psi(L)$.

4.3. The Invariant for Alternating Knots

Before we define a reduced version of $\psi(L)$, we will examine the case of alternating transverse knots. Here, there is a simple condition involving the self-linking number of a transverse knot and its signature, which is sufficient to show the invariant is zero.

Proposition 9. *If K is an alternating, transverse knot then, with respect to the isomorphism in Corollary 2, the odd Plamenevskaya invariant is an element of $\overline{Kh'}_{0,sl(K)+1}(K)$ in the reduced odd Khovanov homology.*

Proof. By Corollary 2, there exists a bigraded abelian group $\overline{Kh'}(K)$ such that

$$Kh'_{m,s}(K) \cong \overline{Kh'}_{m,s-1}(K) \oplus \overline{Kh'}_{m,s+1}(K).$$

Thus, in particular, we have

$$Kh'_{0,sl(K)}(K) \cong \overline{Kh'}_{0,sl(K)-1}(K) \oplus \overline{Kh'}_{0,sl(K)+1}(K).$$

Furthermore, since K is alternating, by [ORSz13, Proposition 5.2] $\overline{Kh'}_{m,s}(K) = 0$ whenever $s - 2m \neq \sigma(K)$. By [Pla06, Corollary 3], for any transverse knot, we have

$sl(K) \leq \sigma(K) - 1$, thus $sl(K) - 1 < \sigma(K)$. Therefore, $sl(K) - 1 \neq \sigma(K)$, and hence

$$\overline{Kh'}_{0,sl(K)-1}(K) = 0.$$

Thus, it follows that

$$Kh'_{0,sl(K)}(K) = \overline{Kh'}_{0,sl(K)+1}(K).$$

Since $\psi(K) \in Kh'_{0,sl(K)}(K)$, the result follows. □

Corollary 3. *For transverse, alternating knot, K, if $sl(K) + 1 \neq \sigma(K)$, then $\psi(K) = 0$.*

Proof. By the previous proposition, $\psi(K) \in \overline{Kh'}_{0,sl(K)+1}(K)$. As in the previous proof, since K is alternating, by [ORSz13, Proposition 5.2], then $\overline{Kh'}_{m,s}(K) = 0$ whenever $s - 2m \neq \sigma(K)$, and thus, since we assume $sl(K) + 1 \neq \sigma(K)$, it follows that

$$\overline{Kh'}_{0,sl(K)+1}(K) = 0.$$

Thus, $\psi(K) = 0$. □

4.4. The Reduced Odd Plamenevskaya Invariant

Definition 3. *As in definition 1, we let α' be the resolution in which the braid representation is separated into b parallel bands. Again, this is the resolution in which there is a 0-smoothing for every positive crossing and a 1-smoothing for every negative crossing. The reduced odd Plamanevskaya invariant $\overline{\psi}(D)$ is a generator of $\Lambda^{b-1}_{\circ} V_{\alpha'}$.*

As with the unreduced invariant, we will abuse notation to refer to both the element in the chain complex and its class in homology (shown to be well-defined in Proposition 10) by $\overline{\psi}(D)$.

Proposition 10. *$\overline{\psi}(D)$ is a cycle.*

Proof. As in showing the unreduced invariant was a cycle, the differential out of $\Lambda^*_\circ V_{\alpha'}$ is 0 or a sum of merges. Without loss of generality, we take a labeling of α' so that the merged circles are a_1 and a_2, and we use

$$\{v_{i-1} - v_i \,|\, 2 \leq i \leq b\}$$

as the basis for $\ker \varphi_{\alpha'}$, generating a basis for $\Lambda^*_\circ V_{\alpha'}$. Then

$$\overline{\psi}(D) = \bigwedge_{i=2}^{b} (v_{i-1} - v_i).$$

Thus

$$\begin{aligned} F_M(\overline{\psi}(D)) &= F_M\left((v_1 - v_2) \wedge \bigwedge_{i=3}^{b} (v_{i-1} - v_i)\right) \\ &= 0 \wedge \bigwedge_{i=3}^{b} (v_{i-1} - v_i) \\ &= 0. \end{aligned}$$

□

Since $\overline{\psi}(D)$ is a cycle, it induces an element in the reduced homology $\overline{Kh'}(L)$. To identify the invariant with the reduced version, we will follow it in the chain complexes explicitly though the identification of $C(D)$ and $\overline{C}(D) \oplus \overline{C}(D)$. We do this below in a series of lemmas. Our proof will use both $\overline{C}(D)$ and $\overline{C}(D \sqcup O)$ where O is an additional unknot labeled a_0. As a braid, the diagram for $D \sqcup O$ is

the diagram for D with an additional strand that is not connected by any crossings. For the vector spaces from which the exterior algebras forming $C(D)$ are built, we will use the notation

$$V_\alpha = \langle v_1, \ldots, v_n \rangle.$$

Each resolution in $C(D)$ corresponds to a resolution in $C(D \sqcup O)$, which will be built out of vector spaces

$$V'_\alpha = \langle v_0, v_1 \ldots, v_n \rangle.$$

We will often use the fact that if $V' = V \oplus \langle v_0 \rangle$, then

$$\Lambda^* V' = \langle \omega, v_0 \wedge \omega \,|\, \omega \in \Lambda^* V \rangle.$$

In Proposition 11, we focus on the invariant defined in the exterior algebra constructed from the resolution α'.

Lemma 6. *There is an isomorphism, Φ_1 between $C(D)$ and $\overline{C}^{(p)}(D \sqcup O)$, where we take $p \in O$.*

Proof. We take a sign assignment on the resolution cube for $C(D)$ and choose the same sign assignment on $C(D \sqcup O)$. This is possible because the squares of each have the same commutativity types. This induces the differential on $\overline{C}^{(p)}(D \sqcup O)$. On the level of the exterior algebras corresponding to each resolution, this comes from a map

$$\phi_1 : \Lambda^* V_\alpha \longrightarrow v_0 \wedge \Lambda^* V'_\alpha.$$

Since $\Lambda^* V'_\alpha = \langle \omega, v_0 \wedge \omega \,|\, \omega \in \Lambda^* V_\alpha \rangle$, then

$$v_0 \wedge \Lambda^* V'_\alpha = \langle v_0 \wedge \omega, v_0 \wedge \omega \,|\, \omega \in \Lambda^* V_\alpha \rangle = \langle v_0 \wedge \omega \,|\, \omega \in \Lambda^* V_\alpha \rangle.$$

Thus, ϕ_1, for $\omega \in \Lambda^* V_\alpha$, is given by

$$\omega \mapsto v_0 \wedge \omega.$$

This extends to all resolutions as a map Φ_1.

Since v_0 is unmodified by the differentials as it corresponds to a circle O which is unaffected by any merges or splits in the corresponding cobordisms, then

$$d(v_0 \wedge \omega) = v_0 \wedge d\omega.$$

Thus, Φ_1 is a chain map. □

Lemma 7. *There is an isomorphism Φ_2 between $\overline{C}^{(p)}(D \sqcup O)$ and $\overline{C}^{(q)}(D \sqcup O)$ where p is a point in O and q is a point in D.*

Proof. This is a consequence of Proposition 8. We have

$$\Phi_2 = (X^q_{D \sqcup O})^{-1} \circ X^p_{D \sqcup O}.$$ □

Lemma 8. *There is an isomorphism, Φ_3 between $\overline{C}^{(q)}(D \sqcup O)$ and $\overline{C}^{(q)}(D) \oplus \overline{C}^{(q)}(D)$.*

Proof. From the exterior algebras, we define

$$\phi_3 : v_1 \wedge \Lambda^* V'_\alpha \longrightarrow (v_1 \wedge \Lambda^* V_\alpha) \oplus (v_1 \wedge \Lambda^* V_\alpha),$$

by observing

$$v_1 \wedge \Lambda^* V'_\alpha = \langle v_1 \wedge \eta, v_0 \wedge v_1 \wedge \eta \,|\, \eta \in \Lambda^* \hat{V} \rangle = \langle \omega, v_0 \wedge \omega \,|\, \omega \in v_1 \wedge \Lambda^* V_\alpha \rangle,$$

so the map is given by

$$\begin{aligned} \omega &\mapsto (\omega, 0) \qquad \omega \in v_1 \wedge \Lambda^* V_\alpha \subset v_1 \wedge \Lambda^* V'_\alpha \\ v_0 \wedge \omega &\mapsto (0, \omega) \qquad \omega \in v_1 \wedge \Lambda^* V_\alpha \subset v_1 \wedge \Lambda^* V'_\alpha. \end{aligned}$$

It is clear that Φ_3 is a chain map. □

Lemma 9. *There is an isomorphism Φ_4 between $\overline{C}^{(q)}(D) \oplus \overline{C}^{(q)}(D)$ and $\overline{C}(D) \oplus \overline{C}(D)$.*

Proof. This is a consequence of Proposition 8. We have

$$\Phi_4 := X_D^q \oplus X_D^q.$$ □

Corollary 4. *There is an isomorphism, $\Phi : C(D) \longrightarrow \overline{C}(D) \oplus \overline{C}(D)$, given by*

$$\Phi := \Phi_4 \circ \Phi_3 \circ \Phi_2 \circ \Phi_1.$$

Note, on the level of the exterior algebras, this corresponds to a map

$$\phi : \Lambda^* V_\alpha \longrightarrow \Lambda^*_\circ V_\alpha \oplus \Lambda^*_\circ V_\alpha$$

given by

$$\phi = (\phi_4 \oplus \phi_4) \circ \phi_3 \circ \phi_2 \circ \phi_1.$$

Proposition 11. *The inclusion map $\overline{Kh'}(L) \hookrightarrow Kh'(L)$ sends the reduced odd Plamenevskaya invariant $\overline{\psi}(D) \in \overline{Kh'}_{0,sl(L)+1}(L)$ to the odd Plamenevskaya invariant $\pm\psi(D) \in Kh'_{0,sl(L)}$.*

Proof. Let α' be the resolution corresponding to the invariant, and let $V'_{\alpha'}$ be the vector space corresponding to the same resolution in $D \sqcup O$, labeled as before. As given in Proposition 8, we define

$$\phi_2 = (\chi^q_{D\sqcup O})^{-1} \circ \chi^p_{D\sqcup O} : v_0 \wedge \Lambda^* V'_{\alpha'} \longrightarrow v_i \wedge \Lambda^* V'_{\alpha'},$$

and

$$\phi_4 = \chi^q_D : v_0 \wedge \Lambda^* V_{\alpha'} : \Lambda^*_\circ V_{\alpha'}.$$

Then,

$$\phi(\tilde{\psi}(D)) = (\phi_4 \oplus \phi_4) \circ \phi_3 \circ \phi_2 \circ \phi_1(\tilde{\psi}(D)).$$

We note that since ϕ_2 is an isomorphism of R-modules that is degree 0 with respect to the natural grading of the exterior algebra, and $v_0 \wedge \tilde{\psi}(D)$ has top degree in the exterior algebra, it follows that

$$\phi_2(v_0 \wedge \tilde{\psi}(D)) = \pm v_0 \wedge \tilde{\psi}(D).$$

Note, $\phi_4 = \chi^q_D$ is an isomorphism of R-modules that is degree -1 with respect to the exterior algebra. Furthermore, $\tilde{\psi}(D) \in v_i \wedge \Lambda^* V_{\alpha'}$ has top degree in the exterior algebra, $\deg_k \tilde{\psi}(D) = b$, and $\tilde{\overline{\psi}}(D)$ has top degree in $\Lambda^*_\circ V_{\alpha'}$, $\deg_k \tilde{\overline{\psi}}(D) = b - 1$. Thus, it follows that

$$\phi_4(\tilde{\psi}(D)) = \pm \tilde{\overline{\psi}}(D).$$

Thus, we have

$$\begin{aligned}
\phi_1 : \quad & \tilde{\phi}(D) & \mapsto \quad & v_0 \wedge \tilde{\psi}(D) \\
\phi_2 : \quad & v_0 \wedge \tilde{\psi}(D) & \mapsto \quad & \pm v_0 \wedge \tilde{\psi}(D) \\
\phi_3 : \quad & \pm v_0 \wedge \tilde{\psi}(D) & \mapsto \quad & (0, \tilde{\psi}(D)) \\
\phi_4 : \quad & \tilde{\psi}(D) & \mapsto \quad & \tilde{\overline{\psi}}(D).
\end{aligned}$$

Therefore,

$$\begin{aligned}
\phi(\tilde{\psi}(D)) &= (\phi_4 \oplus \phi_4) \circ \phi_3 \circ \phi_2 \circ \phi_1(\tilde{\psi}(D)) \\
&= (\phi_4 \oplus \phi_4)(0, \tilde{\psi}(D)) \\
&= (0, \pm\tilde{\overline{\psi}}(D)),
\end{aligned}$$

and thus on the chain complex, we have $\Phi(\tilde{\psi}(D)) = (0, \pm\tilde{\overline{\psi}}(D))$.

Note that $\tilde{\psi}(D) \in \Lambda^b V_{\alpha'}$ and $\Phi(\tilde{\psi}(D)) \in \Lambda^{b-1}(\ker \varphi_{\alpha'})$. Thus

$$\begin{aligned}
\deg_Q \Phi(\tilde{\psi}(D)) &= (\dim \ker \varphi_{\alpha'}) - 2(b-1) + n_+ - 2n_- + |\alpha'| \\
&= (\dim V_{\alpha'} - 1) - 2(b-1) + n_+ - 2n_- + |\alpha'| \\
&= (\dim V_{\alpha'}) - 2b + n_+ - 2n_- + |\alpha'| + 1 \\
&= \deg_Q \tilde{\psi}(D) + 1 \\
&= sl(L) + 1.
\end{aligned}$$

Therefore, $\overline{\psi}(D) \in \overline{Kh'}_{0,sl(L)+1}(D)$. □

Corollary 5. *$\overline{\psi}(D)$ is a transverse link invariant. More precisely, if D and D' are diagrams for a transverse link L, there is a quasi-isomorphism*

$$\overline{\rho} : \overline{C}(D) \longrightarrow \overline{C}(D')$$

such that

$$\overline{\rho}(\overline{\psi}(D)) = \pm\overline{\psi}(D').$$

Proof. Let D and D' both be diagrams for the same transverse link, L. Let

$$\Phi : C(D) \longrightarrow \overline{C}(D) \oplus \overline{C}(D)$$

and

$$\Phi' : C(D') \longrightarrow \overline{C}(D') \oplus \overline{C}(D')$$

be the isomorphisms defined in Corollary 4 for D and D' respectively. Let $\rho : C(D) \longrightarrow C(D')$ be the quasi-isomorphism on the chain complexes given by the invariance of odd Khovanov homology. We have a quasi-isomorphism,

$$\Phi' \circ \rho \circ \Phi^{-1} : \overline{C}(D) \oplus \overline{C}(D) \longrightarrow C(D) \longrightarrow C(D') \longrightarrow \overline{C}(D') \oplus \overline{C}(D')$$

with

$$\Phi' \circ \rho \circ \Phi^{-1}(0, \overline{\psi}(D)) = (0, \pm\overline{\psi}(D')).$$ □

CHAPTER V

PROPERTIES

Proposition 12. *For the standard transverse unknot, O, up to a sign, $\psi(O)$ is a generator of $Kh'_{0,-1}(O) \cong R$.*

Proof. We take the trivial diagram of O. Thus, there are no crossings, and there is only one resolution corresponding to the unique function in $\{0,1\}^{\emptyset}$. The one circle in this resolution is exactly our presentation of O, and it has generator v_0. Thus, we have chain complex

$$0 \longrightarrow \Lambda^*\langle v_0\rangle \longrightarrow 0,$$

and $Kh'_0 = R[-1] \oplus R[1]$. Since $\psi(O) = v_0 \in \Lambda^1\langle v_0\rangle = \langle v_0\rangle = R \cdot v_0$ and its grading is $(0,-1)$, the proof is complete. □

Although trivial, the previous proposition is important to note because ψ is defined first on the level of being a cycle $\tilde{\psi}$ in the chain complex. Thus, it is not immediate that there are links in which $\tilde{\psi}$ is not also a boundary. The following proposition, which is analogous to [Pla06, Propostion 3] however, gives us one condition in which we can guarantee that ψ is a boundary.

Proposition 13. *If L is the negative stabilization of another transverse link, then $\psi(L) = 0$.*

Proof. Assume L is the negative stabilization of another transverse link. Thus for an appropriate choice of braid representation, there is a part of the diagram of L that contains just the negative stabilization with a single negative crossing, and in the chain complex there are two cubes of resolutions corresponding to the 0- and

1-smoothings at this crossing. We will call the diagram D, shown in Figure 38. We note that $d^\star$ here is given by the split cobordism. If we label the circles of D_0 and D_1 that extend beyond the diagram a_1, with corresponding generator v_1, and the circle entirely contained in the diagram of D_1 by a_0, with corresponding generator v_0, then the map $d^\star : D_0 \longrightarrow D_1$ is given by $\omega \mapsto (v_0 - v_1) \wedge \omega$. Note that $\tilde{\psi}(L) \in C(D_1)$.

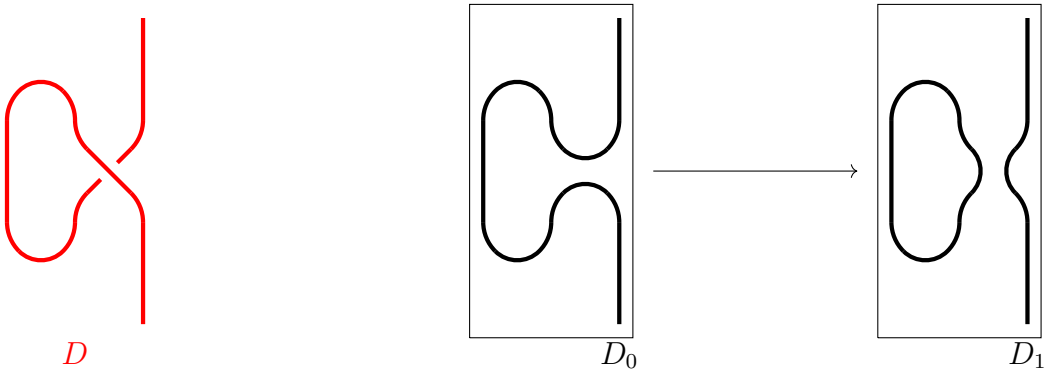

FIGURE 38. **A diagram of D focused on an added negative stabilzation of L, and its resolution cube.**

It suffices to show that $\tilde{\psi}$ is a boundary, so we construct $\tilde{\phi} \in C(D_0)$ such that $d\tilde{\phi} = \tilde{\psi}$. We note that in the cube of resolutions D_1, there is a specific resolution in which $\tilde{\psi}$ resides. We consider the corresponding resolution in D_0. That is, the resolution that has a 0-smoothing at every positive crossing and a 1-smoothing at every negative crossing except the one added by the negative stabilization. If there are n generators $v_1, \ldots, v_n$ in the vector space corresponding to this resolution, then we let $\tilde{\phi} = v_1 \wedge \cdots \wedge v_n$. Note, there is a natural isomorphism between $C(D_0)$, and the chain complex associated to the link L' to which a negative stabilization was added. Up to a sign, our constructed element is the image of $\psi(L')$ under this isomorphism.

Computing $d\tilde{\phi}$, we note there are two sources where the resolution for L has 0-smoothings: the positive crossings of L and the negative crossing introduced by the negative stabilization. On the positive crossings, given our braid representation, a change from a 0-smoothing to a 1-smoothing corresponds to a merge cobordism. Thus, on each summand in the differential $\tilde{\phi} \mapsto 0$, as two factors in the wedge product would be identified. Hence,

$$d\tilde{\phi} = d^{\star}\tilde{\phi} = (v_0 - v_1) \wedge \tilde{\phi} = v_0 \wedge v_1 \wedge \cdots \wedge v_n = \tilde{\psi}. \qquad \square$$

The following proposition is an analog of [Pla06, Theorem 4]. However, as it is not yet know if the odd Khovanov homology is functorial, the proposition below is necessarily weaker.

Proposition 14. *Suppose we have a transverse link L with diagram D, and L_0 is the transverse link with diagram D_0 obtained by replacing a positive crossing in L with the 0-smoothing. There is a homomorphism,*

$$p : Kh'(L) \longrightarrow Kh'(L_0)$$

such that $p(\psi(L)) = \pm\psi(L_0)$.

Proof. In Figure 39, we have the composition of the cobordism from attaching a 1-handle on one side of the positive crossing, and the (R1) move to undo the twist. We examine the diagram of the cobordism in the vertex of the resolution cube in which $\psi(D)$ resides (Figure 39: top), and the corresponding resolutions of D_0 (Figure 39: bottom) both with and without the extra twist by (R1).

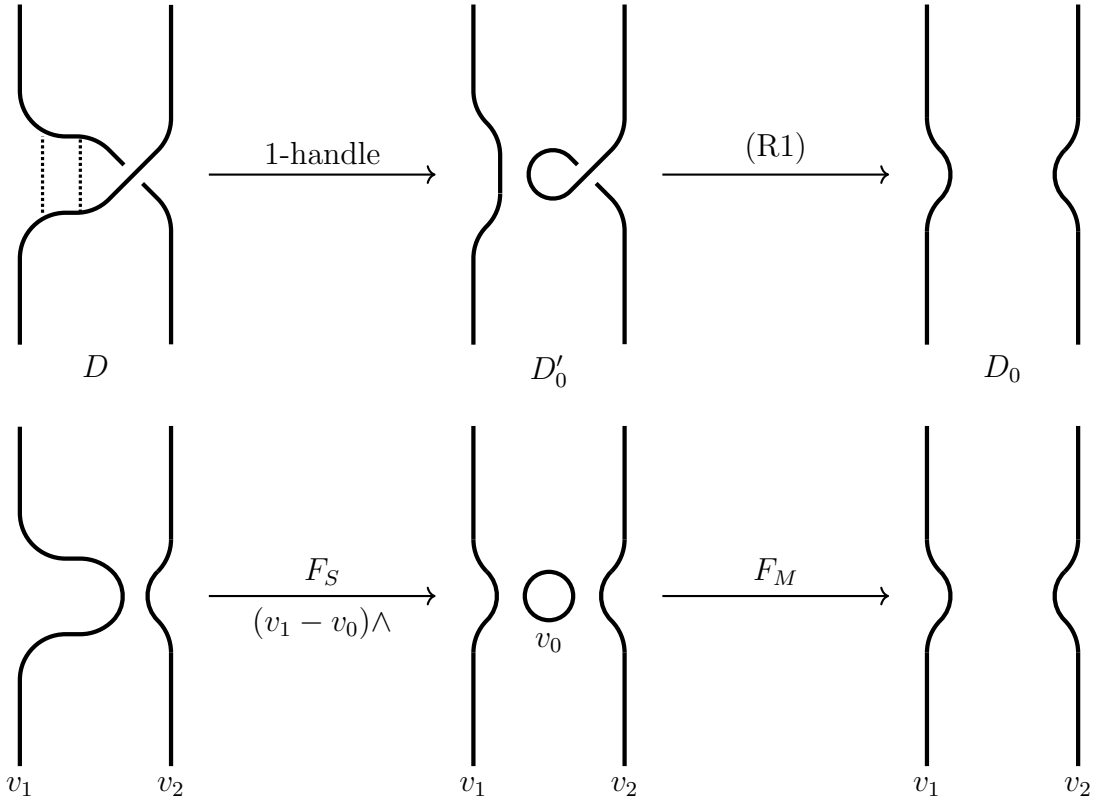

FIGURE 39. **Diagram in vertex for $\psi(D)$.** Top: the cobordism of the 0-smoothing to remove a positive crossing. Bottom: the corresponding resolution complex.

Since the first part of the composition comes from the split cobordism, we have

$$\begin{aligned} F_S(\psi(D)) &= F_S(v_1 \wedge v_2 \wedge \dots) \\ &= (v_1 - v_0) \wedge (v_1 \wedge v_2 \wedge \dots) \\ &= -v_0 \wedge v_1 \wedge v_2 \wedge \dots \\ &= -\psi(D'_0) \end{aligned}$$

and, as we have already seen in Proposition 3

$$= \pm\psi(D_0). \qquad \square$$

Corollary 6. *If L can be represented by a quasi-positive braid, then $\psi(L) \neq 0$.*

CHAPTER VI

COMPUTATIONS

6.1. The Computer Program

To investigate the invariant, the author has written a suite of modules in Python. First, there is the module `braid.py`, with a `Braid` class that represents braids by their braid word as a list of signed integers where the absolute value of each integer represents the left strand of the crossing, and the sign of the integer is the sign of the crossing. For example, the knot 9_{32} is the closure of the braid with braid word

$$\sigma_3^2\sigma_2^{-1}\sigma_3\sigma_2^{-1}\sigma_1\sigma_3\sigma_2^{-1}\sigma_1.$$

In the `Braid` class, this is represented as the list `[3,3,-2,3,-2,1,3,-2,1]`. Below, we have an interaction running `python3` on the command line from the folder containing the modules.

```
>>> import braid
>>> chiral_knot = braid.Braid([3,3,-2,3,-2,1,3,-2,1])
>>> mirror_chiral_knot = chiral_knot.mirror()
>>> reverse_chiral_knot = chiral_knot.reverse()
>>> chiral_knot.self_linking_number()
0
```

The class also uses the author's `braidresolution.sty` package to produce braid diagrams for LaTeX documents. Continuing from above, the command below produces TeX for the diagram in Figure 40.

```
>>> chiral_knot.tex_braid()
```

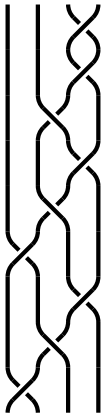

FIGURE 40. **The diagram of** `chiral_knot` **produced by the** `Braid` **class.**

The class also has the addition operator overloaded to compute the connect sum of the closure of two braids.

```
>>> right_trefoil = braid.Braid([1,1,1])
>>> left_trefoil = right_trefoil.mirror()
>>> left_trefoil.get_word()
[-1,-1,-1]
>>> connect_sum = right_trefoil + left_trefoil
>>> connect_sum.get_word()
[1,1,1,-2,-2,-2]
```

The `grid.py` module has a `Grid` class that represents grid diagrams as a pair of lists of integers. The first list gives the column index of the X positions row by row, and the second gives the O positions indexed from 0. By default, the class creates the braid object for the right-heading braid, but it can do so for any direction in the diagram.

```
>>> import grid
>>> trefoil_grid = grid.Grid([3,1,0,4,5,2],[0,5,2,1,3,4])
>>> trefoil_braid = trefoil_grid.braid()
>>> trefoil_braid.get_word()
```

```
[-1, -2, 1, 2, 2, -1]
>>> trefoil_leftward_braid = trefoil_grid.braid('left')
>>> trefoil_leftward_braid.get_word()
[1, -2, 1, -2]
```

The `Grid` class also has methods to produce TEX for the grid diagram, (e.g., `trefoil_braid.tex_grid()`, see Figure 41(a)), the corresponding knot diagram (e.g., `trefoil_braid.tex_knot()`, see Figure 41(b)), and the Legendrian front of the grid (e.g., `trefoil_braid.tex_Legendrian_front()`, see Figure 41(c)).

Corresponding to a diagram with n indexed crossings, there is a resolution cube with 2^n vertices. In the program, these vertices are represented as an integer whose binary representation has i^{th} digit b_i. Thus, a vertex then has the resolution with the b_i-smoothing at the i^{th} crossing for all i, and data corresponding to the vertices is stored in lists whose indices correspond directly to vertices. For the additional information in the resolution cube, we have the `cube.py` module, which contains three classes: the `EdgeStruct` class, the `SquareStruct` class, and the `Vertical` class.

The `EdgeStuct` class is a container for the edges of the resolution cube. In memory, edges are stored as a pair of integers: the vertex of the start of the edge as described above, and the crossing index (indexed from 0), which changes from 0 to 1. This container is used to store both the maps between vertices and the sign assignment, which makes the faces anticommutative. An `EdgeStruct` object also provides an iterator that iterates through the edges primarily in order of the vertices and secondarily in order of the crossing index.

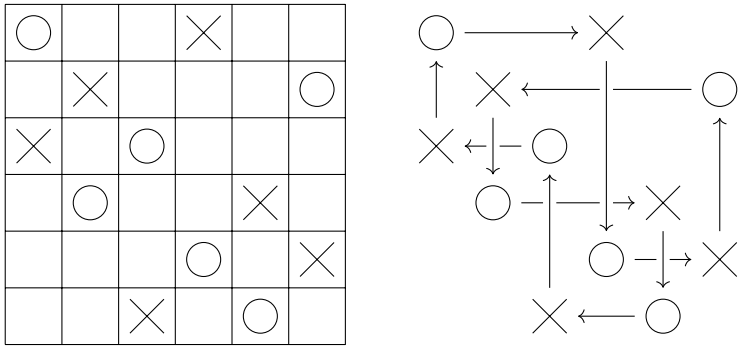

(a) the grid diagram. (b) the knot diagram.

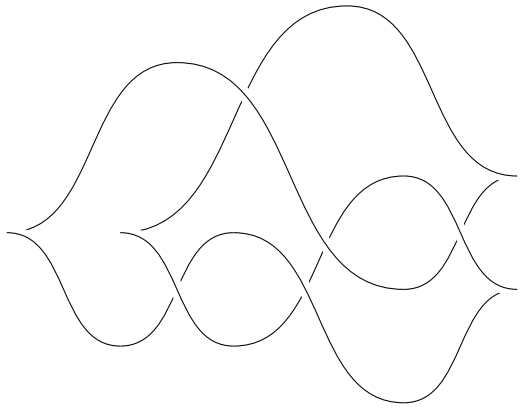

(c) the Legendrian front.

FIGURE 41. **The diagrams of** `chiral_knot` **produced by the** `Grid` **class.**

The `SquareStruct` class is a container for the faces (or squares) of the resolution cube. In memory, squares are stored as a triple of integers: the leftmost vertex in the square, and the two integers representing the two edges in the square that adjoin the leftmost vertex. In the program, there is one `SquareStruct` object that is used as an iterator, but it also acts as a container that stores

information about the commutativity type of the square. The order in which it iterates through the squares is fundamentally different from the `EdgeStuct` class. Since any $(n+1)$-dimensional cube can be represented as two n-dimensional subcubes (one shifted over to the right one spot) connected by 2^n additional edges, the edges' signs are computed inductively from squares on the subcubes. The iterator provided by an `EdgeStruct` objector encodes this inductive order.

The `Vertical` class provides an iterator through all of the generators of the vertex modules that sum to each module in the chain complex. This class is used to produce the matrices from which the homology and the invariant are computed.

There is also the `khovanovhomology.py` module, which contains the `KhovanovHomology` class. This class is both a container that stores the homological information and contains a collection of the methods necessary to compute it. The methods include those which can compute the even and odd Khovanov homologies over $\mathbb{Z}$ and any field, as well as Plamenevskaya's invariant and its odd analog defined in Chapter III. As even and odd Khovanov Homology are categorifications of the Jones polynomial, in the process of computing the resolutions, the `KhovanovHomology` class can calculate the Jones polynomial.

To support these, there are two more modules: `fields.py` and `algebra.py`. The `fields.py` module contains a class FE that handles elements in $\mathbb{Q}$ or $\mathbb{Z}/p$. The benefit of having a single class for field elements of all characteristics is that only a single number needs to be changed to compute the even and odd Khovanov homologies and invariants over different fields. The `algebra.py` module contains a variety of basic supporting functions as well as implementations of different algorithms necessary for computational homology. For an integer matrix A, there is a function that computes its Smith normal form: a

matrix D that is zero except on its diagonal and $D_{i,i}$ divides $D_{i+1,i+1}$, as well as the unimodular matrices S and T such that

$$SAT = D.$$

These output can be used for the inputs of another function that finds the smallest positive n such that

$$Ax = ny$$

if such an n exists. The former function, along with another function that handles row reduction over a field, provide the computations necessary to compute the homology. The latter is used to compute if the invariant is zero and if it is torsion.

In the next example, we show how to generate the odd Khovanov homology for a knot for its grid diagram. Below, we compute the odd Khovanov homology for 8_{19}.

```
>>> import grid
>>> G = grid.Grid([0,1,6,2,5,7,8,3,4,9],[6,7,8,9,1,4,5,0,2,3])
>>> G.comp_full_graded_homology()
>>> B = G.braid()
>>> B.comp_full_graded_homology()
KH'_( 0)(L) = Z^1[ 7] + Z^1[ 5]
KH'_( 1)(L) = 0
KH'_( 2)(L) = Z^1[11] + Z^1[ 9]
KH'_( 3)(L) = 0
KH'_( 4)(L) = Z/2[13] + Z/2[11]
KH'_( 5)(L) = Z^1[17] + (Z^1 + Z/3)[15] + Z/3[13]
Wide knot, sigma = 6, sl = 5.
```

While computing the invariant, the code checks if the invariant is zero in homology, and if not, if it is torsion. Below, we have the computation that shows that the invariant does not distinguish the pair of knots in [BM06, $m10_{140}$]

```
>>> import grid
>>> L1 = grid.Grid([8,7,1,3,5,4,2,6,0],[3,2,4,6,8,7,0,1,5])
>>> B1 = L1.braid()
>>> B1.comp_inv()
Inv NonZero
```

```
>>> L2 = grid.Grid([8,7,0,3,5,4,6,1,2],[3,1,4,6,8,7,2,5,0])
>>> B2 = L2.braid()
>>> B2.comp_inv()
Inv NonZero
```

6.2. Computational Observations

If $\sigma(K)$ is the signature of a knot, then in the knots that have been examined so far, the knots in which the invariant is nonzero correspond exactly with knots in which

$$sl(K) = \sigma(K) - 1.$$

As seen before, if K is alternating, then

$$sl(K) \leq \sigma(K) - 1,$$

thus the invariant is nonzero in the cases where this maximum is reached. This is supported by Proposition 13, which implies of $\psi(K) \neq 0$ then K is not the negative stabilization of another knot. If it were, there would be a knot K' which had the same topological knot type as K, but $sl(K') = sl(K) + 2$.

The even and odd Plamenevskaya invariants are zero and nonzero in the same knots for knots examined.

If n is the length of the braid used in the computation (the number of crossings), and n_- is the number of negative crossings, the invariant is usually zero if $n_-/n > 0.25$, and usually nonzero if $n_-/n < 0.25$. There are a limited number of exceptions, namely the following, which are zero,

$$\begin{aligned} 9_{11}: &\quad [3,3,3,3,-2,1,3,-2,1] && n_-/n = 0.\overline{2}, \\ m9_{20}: &\quad [3,3,3,-2,1,3,-2,1,1] && n_-/n = 0.\overline{2}, \end{aligned}$$

and this one, which is nonzero,

$$m9_{35}: \quad [4,4,3,-4,3,3,2,1,-3,-3,-2,1,3,2] \quad n_-/n = 0.\overline{285714}.$$

Note, for all braids computed, at least one of $\psi(B)$ or $\psi(mB)$ is zero.

So far, the invariant has not been shown to be effective. The Plamenevskaya invariant has not been shown to be effective either, and there is also evidence that it might not be. However, among the reasons why an odd analog of Plamenevskaya's invariant could be effective even if Plamenevskaya's invariant is not is the construction of odd Khovanov homology. Ozsváth and Szabó constructed a spectral sequence whose E_2 term is $KH(L;\mathbb{Z}/2)$, which converges to $\widehat{HF}(L)$ [OSz05]. Attempts to lift the spectral sequence to $\mathbb{Z}$ failed, but inspired the definition of the odd Khovanov homology, where it is conjectured that there is a spectral sequence whose E_2 term is $KH'(L;\mathbb{Z})$ that converges to $\widehat{HF}(\Sigma(mL))$. Ng, Ozsváth and Thurston showed the filtered homotopy type of $\widehat{HF}$, called knot Floer

homology, could be used to distinguish pairs of transverse knots with the same classical transverse invariants. Tracing the Plamenevskaya invariant through to the knot Floer homology is limited by the $\mathbb{Z}/2$ coefficients, however the even analogue is not. We can also compare this to a similar spectral sequence from odd Khovanov homology to the framed instanton homology of the branched double cover of a link [Sca15] and the contact invariant in instanton Floer homology [BS16].

REFERENCES CITED

[AB27] James W. Alexander and Garland B. Briggs. On types of knotted curves. *Ann. of Math. (2)*, 28(1-4):562–586, 1926/27.

[Ale23] James W. Alexander. A lemma on systems of knotted curves. *Proc. Nat. Acad.*, 9(3):93–95, 1923.

[Ben83] Daniel Bennequin. Entrelacements et équations de Pfaff. In *Third Schnepfenried geometry conference, Vol. 1 (Schnepfenried, 1982)*, volume 107 of *Astérisque*, pages 87–161. Soc. Math. France, Paris, 1983.

[Blo10] Jonathan M. Bloom. Odd Khovanov homology is mutation invariant. *Math. Res. Lett.*, 17(1):1–10, 2010.

[BM06] Joan S. Birman and William W. Menasco. Stabilization in the braid groups. II. Transversal simplicity of knots. *Geom. Topol.*, 10:1425–1452, 2006.

[BS16] John A. Baldwin and Steven Sivek. A contact invariant in sutured monopole homology. *Forum Math. Sigma*, 4:e12, 82, 2016.

[BS18] John A. Baldwin and Steven Sivek. Invariants of Legendrian and transverse knots in monopole knot homology. *J. Symplectic Geom.*, 16(4):959–1000, 2018.

[Dar82] Gaston Darboux. Sur le problème de Plaff. *Bull. Sci. Math.*, 6(2):14–36, 1882.

[EH01] John B. Etnyre and Ko Honda. On the nonexistence of tight contact structures. *Ann. of Math. (2)*, 153(3):749–766, 2001.

[EH05] John B. Etnyre and Ko Honda. Cabling and transverse simplicity. *Ann. of Math. (2)*, 162(3):1305–1333, 2005.

[Etn05] John B. Etnyre. Legendrian and transversal knots. In William Menasco and Morwen Thistlethwaite, editors, *Handbook of knot theory*, pages 105–185. Elsevier B. V., Amsterdam, 2005.

[Etn06] John B. Etnyre. Contact manifolds. In Jean-Pierre Françoise, Gregory L. Naber, and Tsou Sheung Tsun, editors, *Encyclopedia of mathematical physics.*, volume 1, pages 631–636. Academic Press/Elsevier Science, Oxford, 2006.

[Gei01] Hansjörg Geiges. A brief history of contact geometry and topology. *Expo. Math.*, 19(1):25–53, 2001.

[Jac04] Magnus Jacobsson. An invariant of link cobordisms from Khovanov homology. *Algebr. Geom. Topol.*, 4:1211–1251, 2004.

[Kan18] Sungkyung Kang. A transverse knot invariant from $\mathbb{Z}_2$-equivariant Heegaard Floer cohomology. https://arxiv.org/abs/1802.00351, February 2018.

[Kho05] Mikhail Khovanov. Categorifications of the colored Jones polynomial. *J. Knot Theory Ramifications*, 14(1):111–130, 2005.

[Kho06] Mikhail Khovanov. An invariant of tangle cobordisms. *Trans. Amer. Math. Soc.*, 358(1):315–327, 2006.

[KN10] Tirasan Khandhawit and Lenhard Ng. A family of transversely nonsimple knots. *Algebr. Geom. Topol.*, 10(1):293–314, 2010.

[Lee03] Eun Soo Lee. *A new structure on Khovanov's homology*. ProQuest LLC, Ann Arbor, MI, 2003. Thesis (Ph.D.)–Massachusetts Institute of Technology.

[Lee05] Eun Soo Lee. An endomorphism of the Khovanov invariant. *Adv. Math.*, 197(2):554–586, 2005.

[LNS15] Robert Lipshitz, Lenhard Ng, and Sucharit Sarkar. On transverse invariants from Khovanov homology. *Quantum Topol.*, 6(3):475–513, 2015.

[LOSSz09] Paolo Lisca, Peter Ozsváth, András I. Stipsicz, and Zoltán Szabó. Heegaard Floer invariants of Legendrian knots in contact three-manifolds. *J. Eur. Math. Soc. (JEMS)*, 11(6):1307–1363, 2009.

[Mar36] Andrei A. Markov. Über die freie Äquivalenz der geschlossenen Zöpfe. *Rec. Math. Moscou*, 43(1):73–78, 1936.

[Mar71] J. Martinet. Formes de contact sur les variétés de dimension 3. In *Proceedings of Liverpool Singularities Symposium, II (1969/1970)*, volume 209, pages 142–163, 1971.

[MOS09] Ciprian Manolescu, Peter Ozsváth, and Sucharit Sarkar. A combinatorial description of knot Floer homology. *Ann. of Math. (2)*, 169(2):633–660, 2009.

[Ng11] Lenhard Ng. Combinatorial knot contact homology and transverse knots. *Adv. Math.*, 227(6):2189–2219, 2011.

[NOT08] Lenhard Ng, Peter Ozsváth, and Dylan Thurston. Transverse knots distinguished by knot Floer homology. *J. Symplectic Geom.*, 6(4):461–490, 2008.

[NT09] Lenhard Ng and Dylan Thurston. Grid diagrams, braids, and contact geometry. In *Proceedings of Gökova Geometry-Topology Conference 2008*, pages 120–136. Gökova Geometry/Topology Conference (GGT), Gökova, 2009.

[OSz05] Peter Ozsváth and Zoltán Szabó. On the Heegaard Floer homology of branched double-covers. *Adv. Math.*, 194(1):1–33, 2005.

[ORSz13] Peter S. Ozsváth, Jacob Rasmussen, and Zoltán Szabó. Odd Khovanov homology. *Algebr. Geom. Topol.*, 13(3):1465–1488, 2013.

[OS03] S. Yu. Orevkov and V. V. Shevchishin. Markov theorem for transversal links. *J. Knot Theory Ramifications*, 12(7):905–913, 2003.

[OSzT08] Peter Ozsváth, Zoltán Szabó, and Dylan Thurston. Legendrian knots, transverse knots and combinatorial Floer homology. *Geom. Topol.*, 12(2):941–980, 2008.

[Pla06] Olga Plamenevskaya. Transverse knots and Khovanov homology. *Math. Res. Lett.*, 13(4):571–586, 2006.

[Put10] Krzysztof Putyra. Cobordisms with chronologies and a generalisation of the Khovanov complex. https://arxiv.org/abs/1004.0889, April 2010.

[Ras10] Jacob Rasmussen. Khovanov homology and the slice genus. *Invent. Math.*, 182(2):419–447, 2010.

[Rei27] Kurt Reidemeister. Elementare Begründung der Knotentheorie. *Abh. Math. Sem. Univ. Hamburg*, 5(1):24–32, 1927.

[Sca15] Christopher W. Scaduto. Instantons and odd Khovanov homology. *J. Topol.*, 8(3):744–810, 2015.

[Shu11] Alexander N. Shumakovitch. Patterns in odd Khovanov homology. *J. Knot Theory Ramifications*, 20(1):203–222, 2011.

[Wri02] Nancy Court Wrinkle. *The Markov theorem for transverse knots*. ProQuest LLC, Ann Arbor, MI, 2002. Thesis (Ph.D.)–Columbia University.